Ecology and Environmental Science and Technology Professional Services

Work Order No: 4600004015-WO03

PO NO: 9500008365

Task 2. 3 Final Project Report

In-Depth Data Analysis and Integration of C-43 Water Quality Treatment and Testing Project: Phase I Bioassays and Mesocosms

Prepared for:

South Florida Water Management District

May 27, 2020

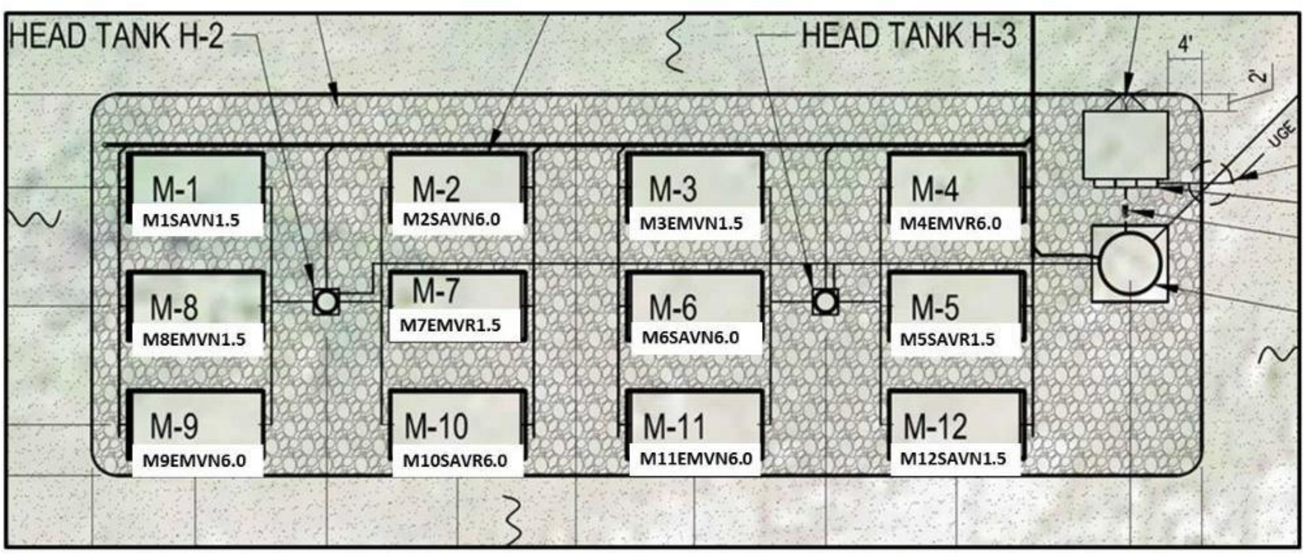

Prepared by:

South Florida Engineering and Consulting LLC

and

Coastal Ecosystems, LLC

May 27, 2020

Cassondra Armstrong, Ph.D.,
Section Administrator of Water Quality Treatment Technologies
South Florida Water Management District
3301 Gun Club Rd,
West Palm Beach, FL 33406
Tel: (561) 682-6716
Email: cthomas@sfwmd.gov

Subject: Task 2.3 Final Project Report: In-Depth Data Analysis and Integration of C-43 Water Quality Treatment and Testing Project: Phase I Bioassays and Mesocosms (4600004015-WO03 - PO NO: 9500008365)

Dear Dr. Armstrong,

South Florida Engineering and Consulting LLC (SFEC) is pleased to submit the Final Project Report as the Task 2.3 deliverable for the above-referenced Work Order. This Final Report summarizes efforts to integrate the Phase I nitrogen removal and cycling components, assess dynamics of dissolved organic nitrogen, and develop nitrogen budgets for the wetland mesocosms at the SFWMD Boma property. The report concludes with proposed recommendations for further consideration during the development of the Phase II of the C-43 Water Quality Treatment and Testing Project.

Respectfully,

Moustafa

Zaki Moustafa, Ph.D.
Principal Scientist/Modeler
30 S M Street, Lake Worth, FL 33460
www.sfec.us
zmoustafa@sfec.us
561-818-8556

ATTACHMENTS:

(1) Final Project Report
(2) Final MS Excel Spreadsheet with 8 N Budgets

Executive Summary

This report describes the results of data analysis and the integration of all components from Phase I of the C-43 Water Quality Treatment and Testing Project (C43-WQTTP) conducted on the Boma Property south of the C-43 Canal. The mesocosm demonstration project evaluated the removal of total nitrogen (TN) by wetlands with different plant communities and hydraulic loading rates (HLR's). The goal of this follow-up work is to conduct an in-depth data analysis of the mesocosm study, including the denitrification and bioassay results, and to construct a mass balance nitrogen cycle model to understand how the created wetlands process, store, and release nitrogen. Importantly, the integrated results from this in-depth evaluation will be used to help inform the study objectives of next phase of the C43-WQTTP research demonstration, Phase II test cells.

The C43-WQTTP had two primary components to determine wetland TN removal using the twelve-tank facility at the Boma Property. The first component (N Removal) quantified the net monthly removal of incoming TN and DON from July 2017 to June 2018. Removal of TN, DON, and dissolved inorganic N (DIN) was categorized by plant community, HLR (1.5 vs. 6.0 cm d^{-1}), and season (dry vs. wet). Half of the tanks had EMV – emergent vegetation while the plant community in the other six was SAV – submerged aquatic vegetation. The second component (N Cycling) quantified internal exchanges of dissolved N between the sediments and water, denitrification (e.g., loss of N through conversion to N2), and sediment decomposition rates in the wet (June 2018) and dry (December 2018) seasons.

A conceptual model of wetland N cycling was created to integrate the physical inputs/outputs of TN (N Removal) with the internal changes in the water and sediments (N Cycling). This approach resulted in a computational scheme to account for the TN removed using the sum of the production and consumption among the internal N pools. The balancing of all N sources vs. sinks revealed the importance of DON as a central but variable part of TN removal. Moreover, DON loss became the key process through which to balance the N budgets. The conceptualization resulted in 9 pools and 14 processes based on the study objectives, the Phase I data and results, and state of knowledge for N cycling in freshwater wetlands.

There was a strong linear relationship observed between TN loading and removal with 27-46% of incoming TN removed by the mesocosms annually. However, only 2-20% of the DON was removed over the same period. This occurred because of reduced DON removal in many wet season months for the mesocosms receiving the lower HLR (1.5 cm d^{-1}). Surplus DON can result in aquatic ecosystems where DIN is in excess of the total N required for net productivity. This pattern was not observed in mesocosms with the higher HLR (6.0 cm d^{-1}). Thus, it was hypothesized that a slightly higher HLR (i.e., HLR $\geq$ 7 cm d^{-1}) could optimize both TN and DON removal by providing the appropriate balance between external DIN loading and internal DON consumption.

Eight N budgets were developed representing each combination of season (dry vs. wet), plant community (EMV vs. SAV), and HLR (1.5 vs. 6.0 cm d^{-1}). The inflows and outflows from the N Removal study were connected to the internal pools of water column DON and DIN. Particulate nitrogen (PN) was assumed to be a single pool of detritus-N located at the sediment-water interface. Similarly, NO_X^- was assumed to be a combined sediment + water N pool because of rapid uptake and denitrification. The exchange of DON and NH_4^+ across the sediment-water interface was measured in the N Cycling component. Algae, plants, and sediments accounted for the remaining N pools. Annual internal primary production was assumed to be in steady state with target biomass estimates. Since some N transformations were not measured in the mesocosms their values were derived during the calibration of the budgets.

Most of the N was located in the algae (6-19% of total), plants (29-82% of total), and PN (8-53% of total) among the eight N budgets. Water column DON was the largest dissolved pool and was nearly double in the SAV budgets compared to the EMV budgets. Denitrification was in excess of combined external NO_x^- loading and internal nitrification in all eight budgets. The biggest difference among all N budgets was the sediment-water DON exchange which ranged from -0.05 gN d^{-1} for sediment influx to 0.36 gN d^{-1} for sediment efflux with no demonstrable relationship to plant community, HLR, or season.

The consumption of DON through photolysis was introduced as a loss term to balance the budgets. The daily rate of photolysis was varied from 1-15% of the internal DON mass to decrease the difference between the target TN removal and the sum of internal cycling. For example, when 10% of the DON was removed daily through photolysis in the SAV 1.5 cm d^{-1} dry season budget, the sum of internal cycling (15.9 gN $season^{-1}$) nearly equaled the target TN removal (16.1 gN $season^{-1}$). However, internal cycling only accounted for 81.7% of the target for the SAV 1.5 cm d^{-1} wet season budget with the same DON loss rate. The four budgets with DON influx to the sediment (EMV 6.0 cm d^{-1} wet , EMV 1.5 cm d^{-1} dry, SAV 1.5 cm d^{-1} wet, and SAV 6.0 cm d^{-1} wet) overestimated the total amount of TN removal by 2.3-7.3% because of internal DON consumption. Conversely, total TN removal was underestimated because of DON efflux from the sediment in the other four budgets (EMV 6.0 cm d^{-1} dry, EMV 1.5 cm d^{-1} wet, SAV 1.5 cm d^{-1} dry, and SAV 6.0 cm d^{-1} dry).

The recommendations for the Phase II test cells were divided into two areas: empirical data and modeling. Assessment of primary production along with the N contents of algae, periphyton, *Utricularia* sp., and plants is necessary to account for internal N sources and sinks. It is essential to characterize TN and DON and evaluate their reactivity under different environmental conditions. In particular, the potential for photolysis as a DON loss term should be thoroughly evaluated. Uncertainty resulting because some N transformations (i.e., uptake, ammonification, nitrification) were estimated rather than determined could be resolved using ^{15}N tracer studies. Introduction of the stable isotope provides a quantitative way to track the N among water, algae, plant, and sediment pools whether using core incubations, mesocosms, or at the scale of the test cells.

The second area for recommendation is to develop a wetland simulation model to evaluate the capacity of the Phase II test cells to filter TN. While the N budgets provided seasonal snapshots of mesocosm N, pools and processes change daily in dynamic models depending upon variable drivers (e.g., temperature, depth, HLR). Sources, sinks, and concentration changes can be examined over multiple scales of time (days-decades) and space (1-1000 m). The ability to predict changes in wetland nutrient storage with expected changes in water management is extremely beneficial. The simulation model can be used to integrate the information gained in Phase II empirical studies and be coupled to operational assessments of the effects of variable HLR, DIN loading, and other variables on wetland TN removal efficiency.

Table of Contents

List of Tables

List of Figures

1 C-43 Watershed

The Caloosahatchee River (C-43 Canal) extends from S-77 at Lake Okeechobee westward through S-78 and S-79 where it transitions to the Caloosahatchee River Estuary (CRE; Figure 1). The area of the C-43 Watershed within the Caloosahatchee River Watershed Protection Plan is approximately 1,000,000 acres with agriculture (34.6%), urban and built up (18.5%), and wetlands (15.9%) as the dominant land uses. The CRE spans approximately 42 km between S-79 and the Sanibel Bridge with the Tidal Basin seaward of S-79 comprising almost 30% of the entire Caloosahatchee Watershed. The C-43 Watershed, Lake Okeechobee, and the Tidal Basin account for 47%, 32%, and 21% of the average total annual freshwater inflow to the CRE, respectively (SFWMD, 2015).

The Basin Management Action Plan (BMAP) for the CRE adopted in November 2012 targeted reduced total nitrogen (TN) loading to the downstream estuary by ~23% (FDEP, 2009; SFWMD, 2015). The stakeholder driven BMAP process focused on identifying watershed restoration projects, which would benefit the overall goal to mitigate nutrient run-off to the CRE. The Comprehensive Everglades Restoration Plan (CERP) includes the West Basin Storage Reservoir Project (CRE-W Res) for the C-43 Watershed. The 10,700 acre reservoir with ~170,000 ac-ft of storage will capture runoff from the C-43 Watershed and Lake Okeechobee outflow in order to (a) reduce excessive discharge to the CRE in the wet season, and, (b) provide freshwater to the estuary during drier periods (SFWMD, 2015; SFWMD, 2018). The construction and implementation of the CRE-W Res could rely on stormwater treatment areas (STA's) to help filter the water exchanged between the reservoir and the C-43 Canal. The C-43 Water Quality Treatment and Testing Project (C43-WQTTP) represents the initial project to accomplish the broader BMAP and CERP goals.

2 C-43 Water Quality Treatment and Testing Project (C43-WQTTP)

2.1 Overview

Phase I of the C43-WQTTP was located on the Boma property, south of the C-43 canal, just upstream of the S-78 control structure (Figure 1). The C43-WQTTP Phase I mesocosm demonstration study was conducted to evaluate the use of wetlands vegetated with different plant communities for the removal of nitrogen from Caloosahatchee surface water (Figure 2). The primary objective of the mesocosm demonstration project was to assess potential surface water nitrogen removal rates using different plant communities, hydraulic loading rates, and soil. More specifically, the project assessed the removal potential for different nitrogen fractions-including the dissolved inorganic species nitrate and ammonia, which are bioavailable to microbes and plants for uptake, and dissolved organic nitrogen (DON), which has unknown bioavailability.

With over 20 years of successful operation of the Everglades Stormwater Treatment Areas, extensive research and expertise in total phosphorus (TP) removal from storm water runoff using wetland treatment systems have been accomplished to date. However, mechanisms for TN removal via wetland treatment systems have not been studied to the same extent and, in fact, are quite limited. The C43-WQTTP Conceptual Plan was completed in 2012 (WSI, 2012), which recommended a phased, multi- scale wetland demonstration testing facility at the Boma property. Under that plan, detailed data review and evaluation of alternative treatment processes initially directed research to the most highly ranked natural treatment options, including constructed wetlands dominated by either emergent vegetation (EMV) or submerged aquatic vegetation (SAV). The phased research demonstration, comprising wetland mesocosms and bioassays (Phase I), followed by test cells and field-scale cells (Phase II), was envisioned to facilitate and establish the basis for design of a future, full-scale constructed treatment facility.

The study targeted the individual removal capacities for ammonium (NH_4^+), nitrate + nitrite (NO_x^-), and particulate and dissolved organic nitrogen (PON and DON) by measuring the changes in nitrogen chemistry of the C-43 water passing through the experimental tanks (J-Tech, 2019). The mesocosm demonstration project also was intended to determine to what extent the proportion of bioavailable DON (BDON) is affected by the different treatments, including a range of hydraulic loading rates. The percentage of bio-available DON (BDON) was evaluated to account for its potential reactivity in aquatic N cycling (Berman and Bronk, 2003; Pisani et al., 2017; J-Tech, 2019). Finally, internal nitrogen biogeochemical processes were determined by incubating intact sediment cores extracted from the mesocosms (Cornwell et al., 2019).

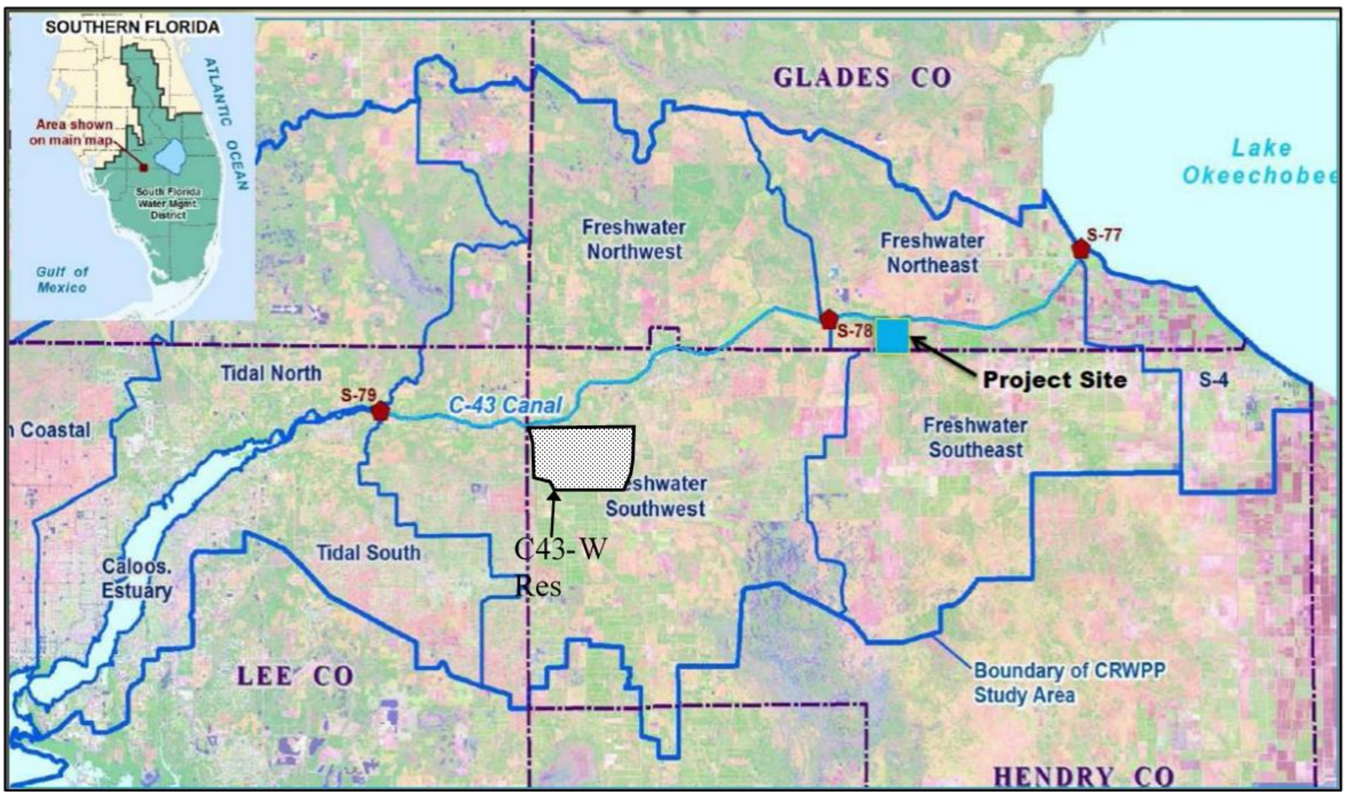

Figure 1. Location map showing Lake Okeechobee, the water control structures (S-77, S-78, S-79), the C-43 Canal, and the site for Phase I of the C-43 Water Quality Treatment and Testing Project (C43-WQTTP) facility at the Boma property

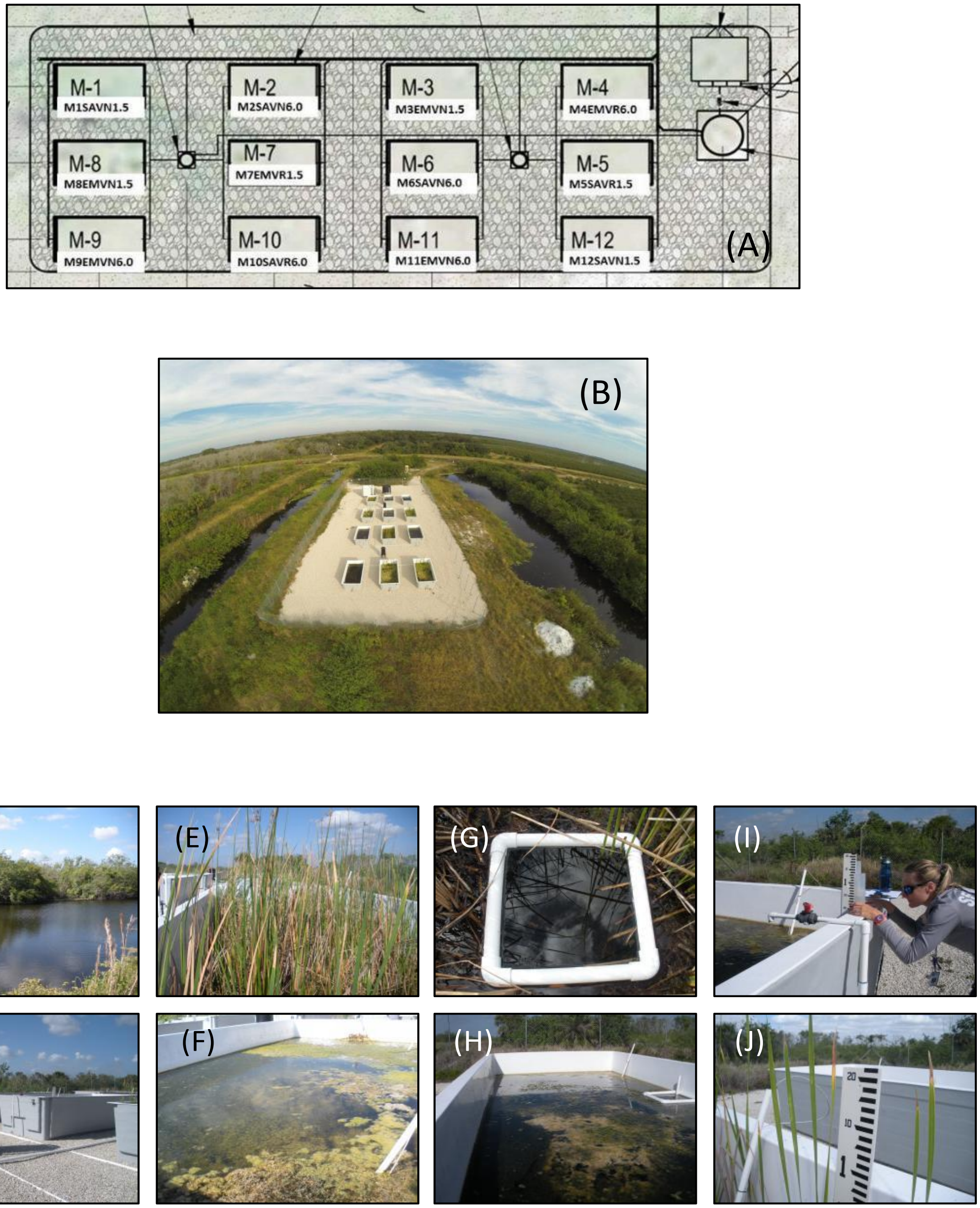

Figure 2. (A) Mesocosm arrangement for the C-43 Water Quality Treatment and Testing Project (C43-WQTTP) facility at the Boma property. (B) Aerial view of the mesocosm setup. (C & D) C-43 Canal and mesocosm set up with large black header tank. (E) Emergent (EMV) mesocosm. (F) Submersed aquatic vegetation (SAV) mesocosm. (G & H) Vegetation sampling grid. (I & J) flow and water level sampling

2.2 N Removal Component Study

The C43-WQTTP Phase I mesocosm demonstration study tested the effects of hydraulic loading rate (HLR: 1.5 vs. 6.0 cm of surface water d^{-1}) and emergent or submersed plant community type (EMV vs. SAV) on wetland N removal. The mesocosm pad was located approximately 2,500 ft south of the C-43 canal with each of the 12 tanks measuring 16' x 8' x 4' for a surface area of 128 ft^2 (11.9 m^2; A_{meso}; J-Tech, 2019). Water was pumped from the C-43 Canal to a large storage tank and then gravity fed to two large opaque secondary header tanks. Each of the secondary tanks provided water to six of the experimental mesocosms (Figure 2).

There was a six-month Start-Up period from July 2016 through December 2016 to allow the plants and sediments to acclimate and stabilize (J-Tech, 2019). The subsequent experimental process was split into three periods: Batch 1, HLR, and Batch 2. The Inflow rates were set at the minimum values to maintain target water levels for each of the tanks throughout each of the two Batch periods. Batch 1 (January 2016 to June 2017) determined the minimum background concentrations of all the nitrogen constituents in the open environment. Steady state water volume was accomplished throughout the HLR by balancing the 1.5 cm d^{-1} or the 6.0 cm d^{-1} inflow with equal outflow volume. The HLR period (July 2017 through June 2018) examined potential effects of plant community and HLR levels on the removal of the nitrogen constituents from the incoming C-43 canal water for an entire year. Batch 2 (July 2018 to December 2018) was used to confirm the initial determination of background concentrations with mature vegetation communities. Finally, the water was sampled during each of the HLR and Batch 2 periods for laboratory bioassays to determine the biologically available BDON (J-Tech, 2019).

The sample sizes were six for the main effects of plant community (EMV vs. SAV) and HLR (1.5 vs. 6.0 cm d^{-1}) and three for the potential interactions (plant X HLR). Water temperature, dissolved oxygen (DO), pH, conductivity, TN, total dissolved nitrogen (TDN), dissolved inorganic nitrogen (DIN = NH_4^+ + NO_x^-), total phosphorus (TP), chlorophyll a, phaeophytin, and turbidity were monitored inside the mesocosms biweekly throughout the experiments (see Table 3in J-Tech, 2019). While periphyton and vegetative cover were monitored monthly, plant biomass and tissue nutrients and a suite of sediment variables (total organic carbon, TP, TN, extractable NH_4^+, bulk density, and percent solids) were determined at the start and end in Batch 1 and semiannually for the 12-month HLR period. Water samples (3 L) were taken from each mesocosm and secondary header tank for laboratory bioassays of BDON twice during the HLR (April and July 2018) and Batch 2 (September and December 2018) periods.

There were no statistically significant effects between plant community (EMV vs. SAV) or HLR (1.5 vs. 6.0 cm d^{-1}) on the removal capacity of any of the N constituents in the mesocosms. While the incoming concentration of TN (TN_{IN}) averaged 1.49 ± 0.03 mg L^{-1}, the outgoing concentration (TN_{OUT}) averaged 1.12 ± 0.02 mg L^{-1} and 1.18 ± 0.02 mg L^{-1} for the EMV and SAV treatments, respectively. These 24% and 22% reductions in the incoming TN concentration equated to removal rates of 0.016 g TN m^{-2} d^{-1} to 0.018 g TN m^{-2} d^{-1} or 32-34% of the incoming N mass. More than 90% of the dissolved inorganic nitrogen (DIN_{IN}) was removed by the wetland mesocosms. DON removal was much lower with DON of approximately 1.0 mg L^{-1} in the outflow (DON_{OUT}). Thus, based on the outgoing concentrations, DON comprised ~87% of the TN leaving the tanks. The DON content of the incoming C-43 canal water was reduced by 3.1-4.4% over the 12-month HLR period. However, DON removal was much greater (~13%)

in the wet season compared to the dry season sampling where some mesocosms exhibited net DON production. Finally, although there was no BDON in DON_{IN}, it was produced internally in the mesocosms (BDON ~ 0.2 mg L^{-1} or ~20% of DON_{OUT}).

2.3 N Cycling Component Study

The objectives of the denitrification study (Cornwell et al., 2019) were to measure denitrification differences between mesocosms, evaluate if the sediments were sources or sinks for nutrients, and test if HLR or plant community affected sediment source vs. sink functionality. Sampling of the mesocosms occurred in June 2018 (HLR) and December 2018 (Batch 2) for this study component. The investigators measured ambient water quality, pore water chemistry, sediment solid phase chemistry, sediment-water dissolved material exchanges, and gaseous fluxes of oxygen (O_2) and di-nitrogen (N_2-N). A total of 60 cores (5 cores x 12 tanks = 60) were incubated in each of the sampling efforts to determine rates of sediment-water exchange. This research group has extensive experience conducting studies of sediment processes and denitrification in aquatic environments (Cornwell et al., 1999; Owens and Cornwell, 2016). Their approach allows the incubation of cores on site in conjunction with the sampling of the water column, aqueous and solid phase sediment properties, vertical exchanges, and denitrification measurements.

Similar to the whole mesocosm N removal study, there were no effects of plant community or HLR on denitrification rates and sediment-water exchanges (Cornwell et al., 2019). However, there was seasonality for many of the observed concentrations and process rates. Levels of organic carbon and nitrogen in the sediments were reduced in December relative to June. Additionally, sediment organic carbon was greater in the EMV relative to the SAV tanks, but only in June. Denitrification rates followed a similar temporal pattern averaging 24.3 ± 29.7 mg N m^{-2} d^{-1} in June and 10.9 ± 11.4 mg N m^{-2} d^{-1} in December. However, the total P content of the sediments, sediment CHLA, and molar C:N did not vary between the two seasonal surveys.

This study indicated that denitrification was the primary mechanism to remove N from the mesocosms (Cornwell et al., 2019). NO_x^- exchange rates were low and mostly into the sediments. N_2-N efflux in the SAV tanks averaged 0.85 ± 0.94 and 0.43 ± 0.29 mg N m^{-2} h^{-1} in June vs. December. Denitrification rates in the EMV tanks were slightly greater in the wet season (1.4 ± 0.88 mg N m^{-2} h^{-1}). The high concentrations of NH_4^+ in the sediment porewater of the SAV (7.5 ± 4.8 mg N L^{-1}) and EMV (1.6 ± 2.2 mg N L^{-1}) mesocosms generally drove the efflux of NH_4^+ from the sediments. While cores incubated in the dark resulted in NH_4^+ production rates of 0.93 ± 0.19 and 0.18 ± 0.54 mg N m^{-2} h^{-1} in June and December, respectively, sediment production of NH_4^+ and N_2-N were less in cores from four of the EMV tanks which required illumination. Primary production by sediment surface microalgae reduces N available to the water column. Sediment surface photosynthesis in illuminated tanks was statistically similar between June (16.6 mg C m^{-2} h^{-1}) and December (13.2 mg C m^{-2} h^{-1}).

DON dynamics were much more variable and difficult to discern than DIN. Although sediment porewater concentrations were relatively high in June (1.6 ± 1.5 mg N L^{-1}) and December (2.6 ± 2.3 mg N L^{-1}), DON exchange rates were highly variable in both magnitude and direction. In fact, the DON exchange rates were non-interpretable in 15 of 60 dark incubation cores in June and 6 of 60 in December (Cornwell et al., 2019). This means that the linear regression derived from the expected change in DON concentration (dependent) over the incubation time (independent) did not have a significant positive or negative slope.

Finally, illumination reduced rates of DON exchange in June but not necessarily in December. Variability and uncertainty regarding DON dynamics in aquatic ecosystems is common (Berman and Bronk, 2003).

Although wetlands maintain their long-term vertical position by balancing organic deposition relative to microbial consumption, rapid N cycling between organic and inorganic pools in the water and sediment is the mechanism which transfers water column N to the sediments. In the case of the mesocosms, denitrification was the primary loss pathway and the sediments were a short-term sink for N (Cornwell et al., 2019). The internal production of organic matter within the mesocosms provided the sediment with a relatively labile pool of which ~2% was demineralized daily. It follows that the turnover rate for sediment organic C (0.01-0.07 d^{-1}) was several times greater than that in natural peat or coastal wetlands. In fact, some analyses of long-term sediment geochemical processes were not possible due to the absence of antecedent organic matter in the experimental mesocosms (Cornwell et al., 2019). The rate at which sediment organic N was converted to N_2 ranged from 0.001-0.008 d^{-1} consuming 0.1% to 0.8% of the sediment pool daily. This means that unlike natural wetlands with antecedent organic matter (i.e. peat), the sediments within the mesocosm tanks would likely be starved of organic matter without sufficient HLR and new internal production.

3 Project Goal and Objectives

The goal of the supplement work under this Work Order (4600004015-WO03) was to conduct an in-depth data analysis of the mesocosm study and to construct a mass balance nitrogen budget to understand how the created wetlands process, store, and release nitrogen. More importantly, the integrated results from Phase I in-depth analyses and evaluation will be used to help guide and shape the objectives of the next phase of the C43-WQTTP study. The specific objectives of the current project were to:

1. Integrate the results of the mesocosm, bioassay, and denitrification studies into one comprehensive assessment of nitrogen dynamics within the different treatments
2. Assess DON dynamics and potential for removal under different operational conditions (season, flow rate, etc.)
3. Create a mass balance model of all available components to reflect the nitrogen cycle in the mesocosms
4. Develop recommendations for additional questions to address in future studies

Addressing these three inter-related objectives provided the pathway to recommendations for additional studies which will benefit the development and operation of the Phase II wetland test cells.

4 Project Description

4.1 Integration of C43WTTP Study Components

4.1.1 Approach

The approach integrated the physical transport (N Removal) with the internal processes and transformations (N Cycling). The total amount of N removed should equal the net change among the internal N constituents in order to account for all N and develop mass balance N budgets. Accounting for the fate of introduced N is fundamental to understanding wetland processes and managing nutrient loads. It was also important to consider that DON in the water and sediments is central to N cycling in aquatic ecosystems (Berman and Bronk 2003). Therefore, integrating the N Removal and N Cycling components was fundamental to analyze DON dynamics and create the seasonal N budgets.

The N Removal study (J-Tech, 2019) quantified the net removal of the incoming TN, DON, and DIN (ΔN_{remove}; gN month^{-1}) at monthly intervals during the 12-month HLR period for each of the 12 mesocosms. The net removal for each N constituent was calculated as the difference between total input (HLR + rain) and the outflow for each tank. Thus, there were 144 values for the inflows from the header tanks, atmospheric inputs, and outflows from the mesocosms. The net monthly removal of TN and DON were categorized wet (May-Oct) season for application to N budgets. The percent composition of TN in the header tanks by plant community (EMV vs. SAV), HLR (1.5 vs. 6.0 cm d^{-1}), and dry (Nov-Apr) or was calculated among the N constituents (TN = DON + NH_4^+ + NO_X^- + PN) to split incoming TN into its components for the N budgets.

The N Removal study determined the concentrations of TN, DON, DIN (NH_4^+ + NO_X^-), and chlorophyll *a* for the water column within each mesocosm. These concentrations and the tank water volumes were used to calculate the mass of N in the water for inclusion in the N budgets. These same data were used to calculate the percent composition of the water column TN within the mesocosms to split outgoing TN into its components for the N budgets. The N Cycling component (Cornwell et al. 2019) quantified internal rates of sediment-water exchanges, denitrification, and sediment decomposition for the wet (June 2018) and dry seasons (December 2018; gN m^{-2} d^{-1}). The data and information derived from this study were essential to specify the internal pools and processes in the conceptual model of N cycling. Although conducted after the 12-month HLR period, pool concentrations and process rates observed in the December sampling were assumed to represent dry season N conditions. Sediment bulk density, total N, and porewater concentrations of DON + NH_4^+ + NO_X^- were used to calculate sediment N pool sizes in the N budgets.

4.2 Conceptual Model

This study relied on a conceptual model of N cycling in freshwater wetlands to integrate the three objectives and guide Phase II recommendations (Figure 3). While the inputs (HLR + rain) and outputs were comparatively easy to establish from the N Removal study, the number of N pools and processes (Table 1) within the wetland mesocosm had to be determined based on the availability of data and understanding of the wetland ecosystem. Although a majority of the information required to construct the N budgets was determined in the two studies, some information was missing (Mass Balance N Budgets).

The inflows and outflows served as sources and sinks, respectively, for DON (DON_w), NH_4^+ ($NH4_w$), NO_X^-, and PN inside the mesocosms. Since it had both external and internal sources, PN was assumed to be a single internal pool of detrital N located at the sediment-water interface. Similarly, NO_X^- was assumed to be a combined sediment + water N pool (NO_{Xsw}) because of fast exchange and denitrification across the interface. Although combined into a single algal N pool (N_{algae}) for display in Figure 3, the water column included separate N pools for phytoplankton (N_{phyto}) and periphyton (N_{peri}) contributing to the PN pool. The remaining pools were for the plants (N_{plant}; EMV or SAV) and DON and NH_4^+ in the sediment porewater (DON_s and $NH4_s$).

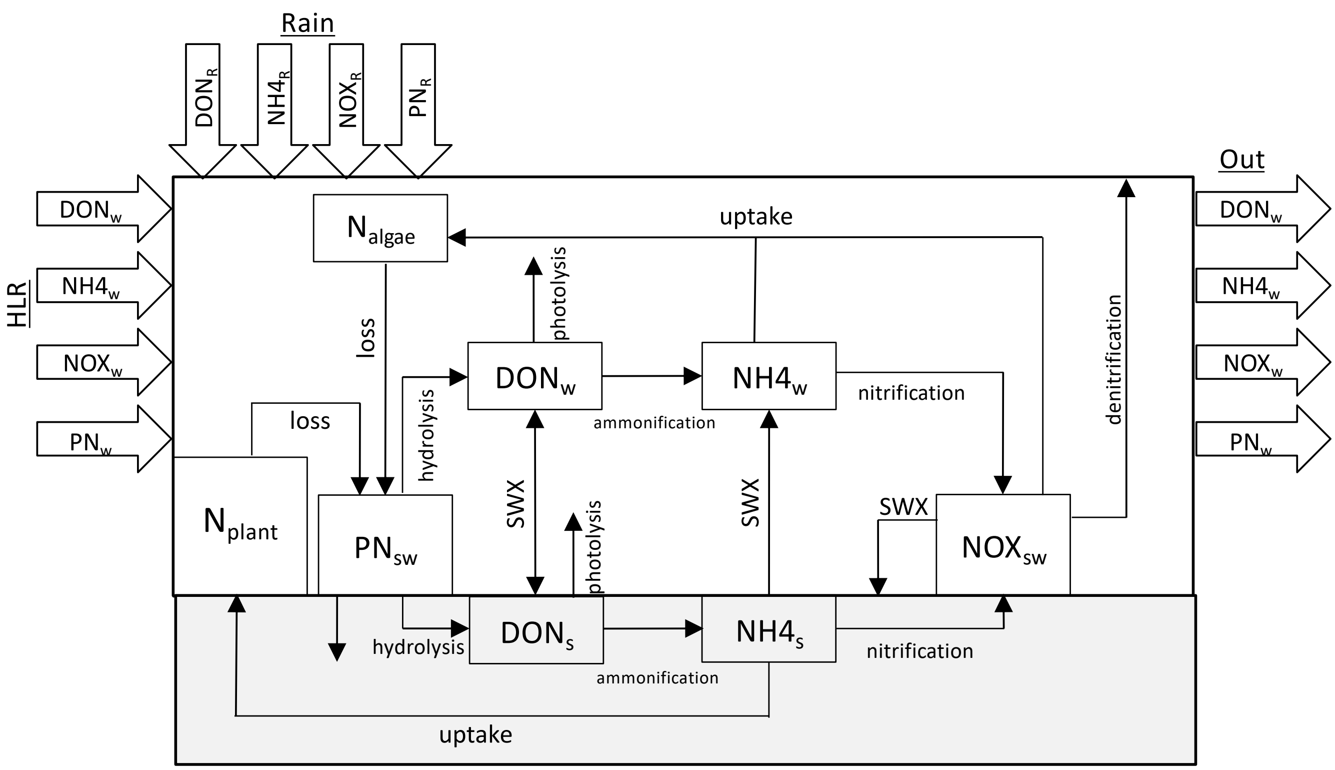

Figure 3. Compartmental diagram to integrate Phase I research components, develop mass balance nitrogen budget, and assess potential differences in TN and DON processing in the experimental mesocosms.

The mortality of phytoplankton, periphyton, and plants (e.g. loss) served as the internal source of PN_{sw} Figure 3. Separate fractions of PN were assumed to undergo hydrolysis as sources of DON to the sediments and water column (DON_w and DON_s). DON at the sediment-water interface (SWX) was either into or out of the sediment depending upon the particular mesocosm and season. Photolysis and ammonification were the primary loss terms for both DON pools. Ammonification was the source term for water column NH4 with SWX and nitrification functioning as sinks. N uptake by plants and algae was specified as a loss term for NH_4 in the sediment and water column, respectively. Denitrification, SWX, and algal uptake were the loss terms for NOX_{sw}.

4.3 TN Mass Balance Computation

This conceptualization led to two separate calculations of mass removal with which to perform a mass balance for TN. The first calculation was total TN removal (ΔTN_{remove}; gN month^{-1}):

$$\Delta TN_{REMOVE} = [TN_{HLR} + TN_{RAIN}] - TN_{OUT}$$

Where the TN sources were HLR (TN_{HLR}) and rain (TN_{RAIN}) and the sink was the outflow (TN_{OUT}). The second calculation ($\Delta TN_{cycling}$; gN month^{-1}) was the sum of the changes to the internal pools:

$$\Delta TN_{CYCLING} = \Sigma[\Delta DON + \Delta NH_4^+ + \Delta NO_X^- + \Delta PN]$$

Thus, if $\Delta TN_{cycling}$ equaled ΔTN_{remove} then the resulting N budget accounted for all of the incoming N. If these values are not equal or close, then not all N was tracked, and the budgets were out of balance.

Table 1. List of pools and processes for mesocosm nitrogen cycle

Nitrogen Pools	Abbrev	Unit	Data Source
Phytoplankton	N_{phyto}	g N	J-Tech, 2019
Periphyton	N_{peri}	g N	J-Tech, 2019
Plants	N_{plant}	g N	J-Tech, 2019
Particulate (water + sediment)	PN_{ws}	g N	J-Tech, 2019
Dissolved Organic (water)	DON_w	g N	J-Tech, 2019
Ammonium (water)	NH_{4w}	g N	J-Tech, 2019
Nitrate + Nitrite (water + sediment)	NO_{Xws}	g N	J-Tech, 2019
Dissolved Organic (sed)	DON_s	g N	J-Tech, 2019; Corrnwell, 2019
Ammonium (sed)	$NH4_s$	g N	J-Tech, 2019; Corrnwell, 2019
Nitrogen Processes			
Periphyton uptake	N_{periup}	g N d^{-1}	Calculated
Phytoplankton uptake	N_{phyup}	g N d^{-1}	Calculated
Plant uptake	$N_{plantup}$	g N d^{-1}	Calculated
Phytoplankton loss	$N_{phytoloss}$	g N d^{-1}	Calculated
Periphyton loss	$N_{periloss}$	g N d^{-1}	Calculated
Plant loss	$N_{plantloss}$	g N d^{-1}	Calculated
Hydrolysis	N_{hydrol}	g N d^{-1}	Buzzelli et al., 2014
Ammonification	N_{ammon}	g N d^{-1}	Buzzelli et al., 2014
Photolysis	N_{photol}	g N d^{-1}	Calibration
Sediment Water Exchanges			
Ammonium	SWX_{NH4}	g N d^{-1}	Cornwell et al., 2019
Nitrate + Nitrite	SWX_{NOx}	g N d^{-1}	Cornwell et al., 2019
Particulate Organic	SWX_{PON}	g N d^{-1}	Cornwell et al., 2019
Dissolved Organic	SWX_{DON}	g N d^{-1}	Cornwell et al., 2019

Note: . See Figure 3 for compartmental diagram for nitrogen cycling. The Algae pool is assumed to include periphyton and *Utricularia*.

4.4 Evaluation of DON Dynamics

4.4.1 Approach

The first step to address this objective was to plot TN loading vs. mesocosm-specific mass (gN month^{-1}) of incoming TN removed monthly to assess the overall relationship. The second step was to examine the time series of the percentage of incoming TN and DON removed for each of the 12 mesocosms over the 12-month HLR period. Differences within and among the time series were contrasted relative to month, plant community type (EMV vs. SAV), HLR (1.5 vs. 6.0 cm d^{-1}). The relationships between external loading and internal DON production were explored for specific months and mesocosms with surplus DON. Finally, a hypothesis was developed to explain DON cycling to optimize its removal during operation of the test cells and/or STA's.

4.4.2 TN and DON Removal

There was a strong linear relationship between TN loading (Q_{TN}; g m^{-2} d^{-1}) and the mass of TN removed by the mesocosms (gN month^{-1}; Figure 4A). Results were clustered representative of 1.5 vs. 6.0 cm d^{-1} HLR treatments. TN loading (Q_{TN}) ranged up to 0.1 g m^{-2} d^{-1} with a maximum TN mass removed of ~18 g month^{-1}. The percentage of incoming TN removed by the mesocosms during the HLR period varied from the most efficient at >40% (M1, M5, M8) to the least effective where only 28-30% of the TN was removed (M2, M6, M7, M11, M12; Table 2).

4.4.3 TN and DON Removal

There was a strong linear relationship between TN loading (Q_{TN}; g m^{-2} d^{-1}) and the mass of TN removed by the mesocosms (gN month^{-1}; Figure 4A). Results were clustered representative of the 1.5 vs. 6.0 cm d^{-1} HLR treatments. TN loading (Q_{TN}) ranged up to 0.1 g m^{-2} d^{-1} with a maximum TN mass removed of ~18 g month^{-1}. The percentage of incoming TN removed by the mesocosms during the HLR period varied from the most efficient at >40% (M1, M5, M8) to the least effective where only 28-30% of the TN was removed (M2, M6, M7, M11, M12; Table 2).

Although TN removal was linear and predictable, DON removal among the mesocosms was not. This inconsistency is central to the biogeochemical and operational uncertainties for wetlands constructed to filter N and a primary emphasis of the current study (Gribsholt et al., 2005; Vyzamal, 2016). It is important because the composition of the TN from both header tanks and the outflow was 83-92% DON (Table 3).

The percentage of incoming DON removed ranged from 2-5% (M3, M4, M6, M7) to 18-19% (M1, M8, M12; Table 2). The mass of DON removed was consistently less than 5 g month^{-1} with 34 occurrences of zero DON consumption or net DON production among the 144 values (Figure 4B). TN removal did not fluctuate nearly as great as DON over the 12-month HLR period from July 2017 to June 2018 (Figure 5). There appeared to be much less temporal fluctuation for mesocosms receiving the 6.0 cm d^{-1} HLR (M2, M4, M6, M9, M10, M11) relative to those with 1.5 cm d^{-1} HLR (M1, M3, M5, M7, M8, M12).

Almost all of the 34 months with zero DON removal or DON production were from the mesocosms receiving the 1.5 cm d^{-1} HLR (Figure 6). The time series for each of these exhibited declines in both TN and DON removal in Sept 2017 and May 2018. Additionally, there were months where increasing DON consumption coincided with decreasing TN removal. Obvious examples occurred in Aug 2017 in M1 and in Nov 2017 for M3, M7, and M12. This suggests that DIN was scarce and almost all of the TN removal was in the form of DON.

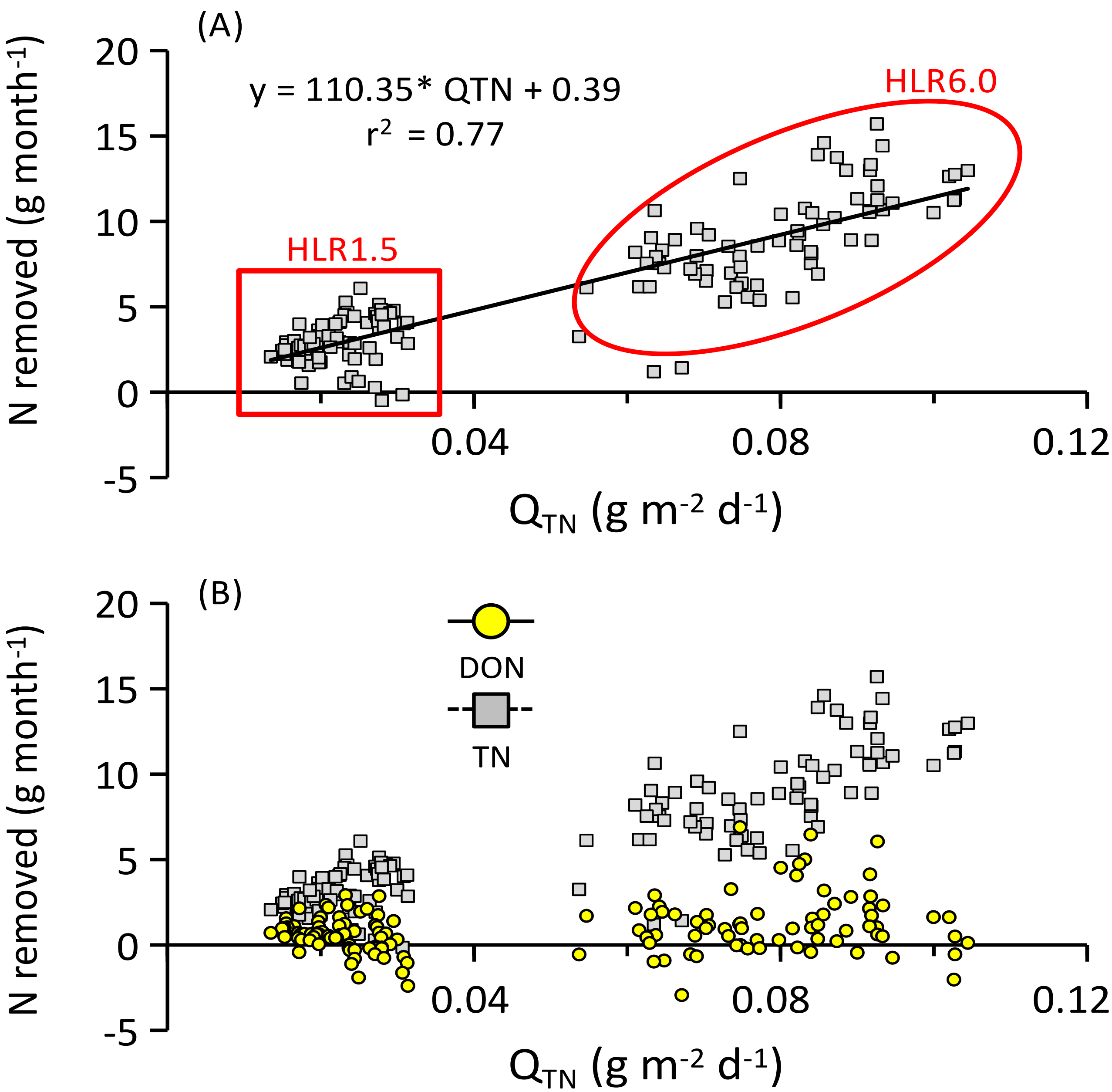

Figure 4. Scatterplots of the TN load (Q_{TN}; g m^{-2} d^{-1}) vs. the monthly mass of N removed from the mesocosms (g $month^{-1}$). (A) TN removal only. (B) TN and DON removal.

Although the incoming TN was generally < 3% DIN, the wetland mesocosms removed 90-97% of the DIN mass (Table 3). Tanks M1, M7, and M12 were the most efficient at ~96% DIN removal (Table 2). These mesocosms each had HLR 1.5 cm d^{-1} and months where nearly all the TN removal was in the form of DON. Although DIN concentrations were generally very low its availability and reactivity are central to DON dynamics in aquatic systems (Berman and Bronk, 2003; Pisani et al., 2017).

Pisani et al., (2017) offered a conceptual model of microbially mediated N processes resulting from their study of DON in the C-43 Canal. The dynamic equilibrium among N_2, DON, NH_4^+, and NO_X^- pools requires the consumption of DON to maintain ecosystem primary production when nutrients are limiting (Figure 7). Based on this model, a microbially dominated aquatic ecosystem with sufficient or excess DIN should result in surplus DON.

In order to test this conceptual model and explain the observed DON production, the monthly percentage of DON removed was plotted vs. the daily DIN loading rate for all 144 data points (Q_{DIN}; g m^{-2} d^{-1}; Figure 8). While the initial plot resulted in two distinct clusters of points indicative of the two HLR's, there appeared to be no overall relationship between Q_{DIN} and DON removal (Figure 7A). However, more detailed analysis of the percent DON removal for mesocosms receiving only 1.5 cm d^{-1} HLR (N = 72) revealed two distinct clusters of points (Figure 8B and Figure 8C). Finally, a clear relationship emerged between increased Q_{DIN} and reduced DON removal efficiency for a sub-set of wet season months where the HLR was 1.5 m d^{-1} (Figure 8C). Thus, relatively high DIN availability under the low HLR coincided with surplus DON production in May and September.

4.4.4 HLR Based Hypothesis for DON Removal

The DON analytical sequence led to the hypothesis that there could be an optimal range for HLR where both TN and DON would be removed with maximum efficiency (Figure 9). This is based on the concept of the chemostat for microbial metabolic experiments (Veldkamp, 1977). Microbially mediated internal N cycling should dominate at very low levels of HLR although ecosystem production might be limited by reduced availability of inorganic N. Both TN and DON removal should be minimal in this scenario. Under very high levels of HLR it is not likely that nutrient cycling within the wetland ecosystem could influence the composition of the water column as materials might simply washout too fast. The balance between physical transport and internal biogeochemical cycling occurs at intermediate HLRs (e.g. flushing times) in many aquatic ecosystems.

It was possible that the HLR of 1.5 cm d^{-1} was low enough to favor internal cycling during certain months (e.g. May and November) at the same time that the internal production of DIN was potentially greater within the mesocosms. In other words, the increased availability of DIN from combined external loading and internal production under the HLR 1.5 cm d^{-1} reduced DON consumption thus validating the Pisani et al (2017) hypothesis. While these apparent patterns were not as obvious for the more quickly flushed mesocosms receiving HLR 6.0 cm d^{-1}, there were slight declines in TN removal in May and Sept in some cases (Figure 5). Thus, it is hypothesized that an optimal HLR range of 7-8 cm d^{-1} could optimize both TN and DON removal in the test cell or STA. This equated to ~7-8-day flushing time for the mesocosms.

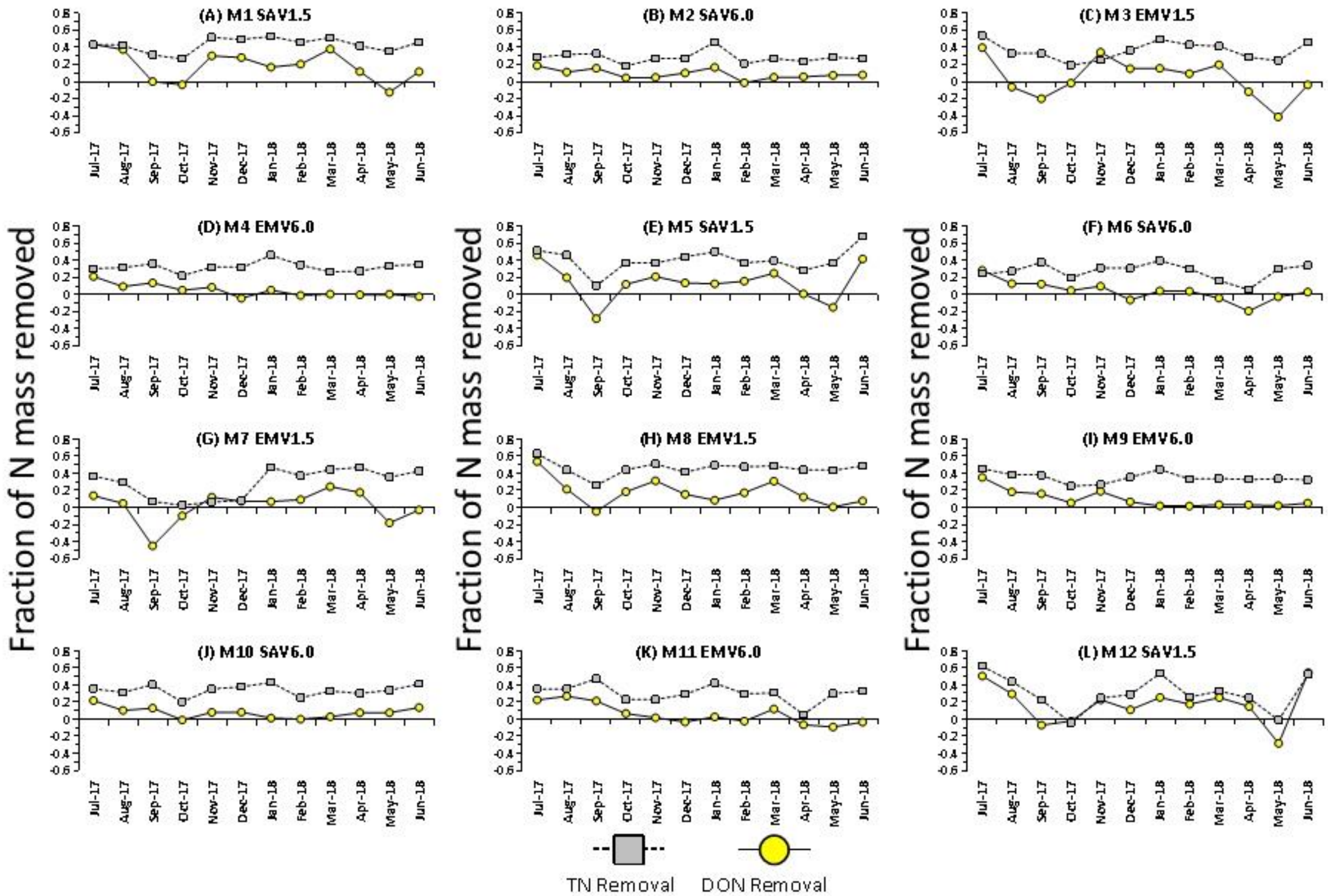

Figure 5. Time series of the monthly fraction of TN (dash/grey square) and DON (solid/yellow circle) for each of the twelve mesocosms (A-L).

Table 2. Removal of total nitrogen (TN), dissolved organic nitrogen (DON), and dissolved inorganic nitrogen (DIN) by each of the 12 mesocosms over the 12-month HLR period. Provided are the total annual changes (g N y^{-1}) in each of the masses (ΔTN, ΔDON, ΔDIN) and the percentages of incoming TN, DON, and DIN removed over the 12 months (%TN, %DON, %DIN). Mesocosms had either emergent vegetation (EMV) or submersed aquatic vegetation (SAV) communities (plant) and were subjected to two hydraulic loading rates (HLR) (1.5 vs. 6.0 cm d^{-1}).

Mesocosm	Plant	HLR	ΔTN	%TN	ΔDON	%DON	ΔDIN	%DIN
1	SAV	1.5	40.3	43%	10.1	19%	30.2	96%
2	SAV	6	99.1	28%	27.7	9%	76.8	90%
3	EMV	1.5	35.5	36%	2.3	4%	30	95%
4	EMV	6	115.9	32%	11.8	5%	79.6	94%
5	SAV	1.5	39.2	41%	8.1	14%	29.1	94%
6	SAV	6	93.7	27%	10.9	4%	75.6	94%
7	EMV	1.5	27.7	29%	0.6	2%	30.2	94%
8	EMV	1.5	44.5	46%	10	18%	30.6	96%
9	EMV	6	118.9	35%	22	10%	79.2	94%
10	SAV	6	117.2	34%	17.7	8%	78.7	92%
11	EMV	6	105.5	30%	13.1	6%	76.3	93%
12	SAV	1.5	29.4	30%	10.4	18%	30.8	97%

Table 3. Average percentages for dissolved organic nitrogen (%DON), ammonium (%NH_4), nitrate + nitrite (%NO_X), and particulate nitrogen (%PN) of incoming total nitrogen (TN) from the header tanks (IN) and outgoing total nitrogen (OUT) for each combination of plant community (EMV vs. SAV) and hydraulic loading rate (HLR 1.5 vs. 6.0 cm d^{-1}).

Plant	HLR	Season	%DON IN	%NH4 IN	%NOX IN	%PN IN	%DON OUT	%NH4 OUT	%NOX OUT	%PN OUT
EMV	1.5	Dry	88.2	1.7	0.3	9.8	87.4	1.7	0.3	10.6
EMV	1.5	Wet	85.4	2.1	0.3	12.2	85.3	2.1	0.3	12.3
EMV	6.0	Dry	92	1.9	0.5	5.6	90.7	1.9	0.5	6.9
EMV	6.0	Wet	86.4	2.1	0.4	11.1	86.3	2.1	0.3	11.3
SAV	1.5	Dry	85.1	1.6	0.5	12.9	83.9	1.5	0.5	14.1
SAV	1.5	Wet	72	1.7	0.2	26.1	70.9	1.6	0.2	27.3
SAV	6.0	Dry	89.2	2	0.3	8.5	89.1	2	0.3	8.7
SAV	6.0	Wet	83.1	2.9	0.2	13.7	83	2.9	0.2	13.9

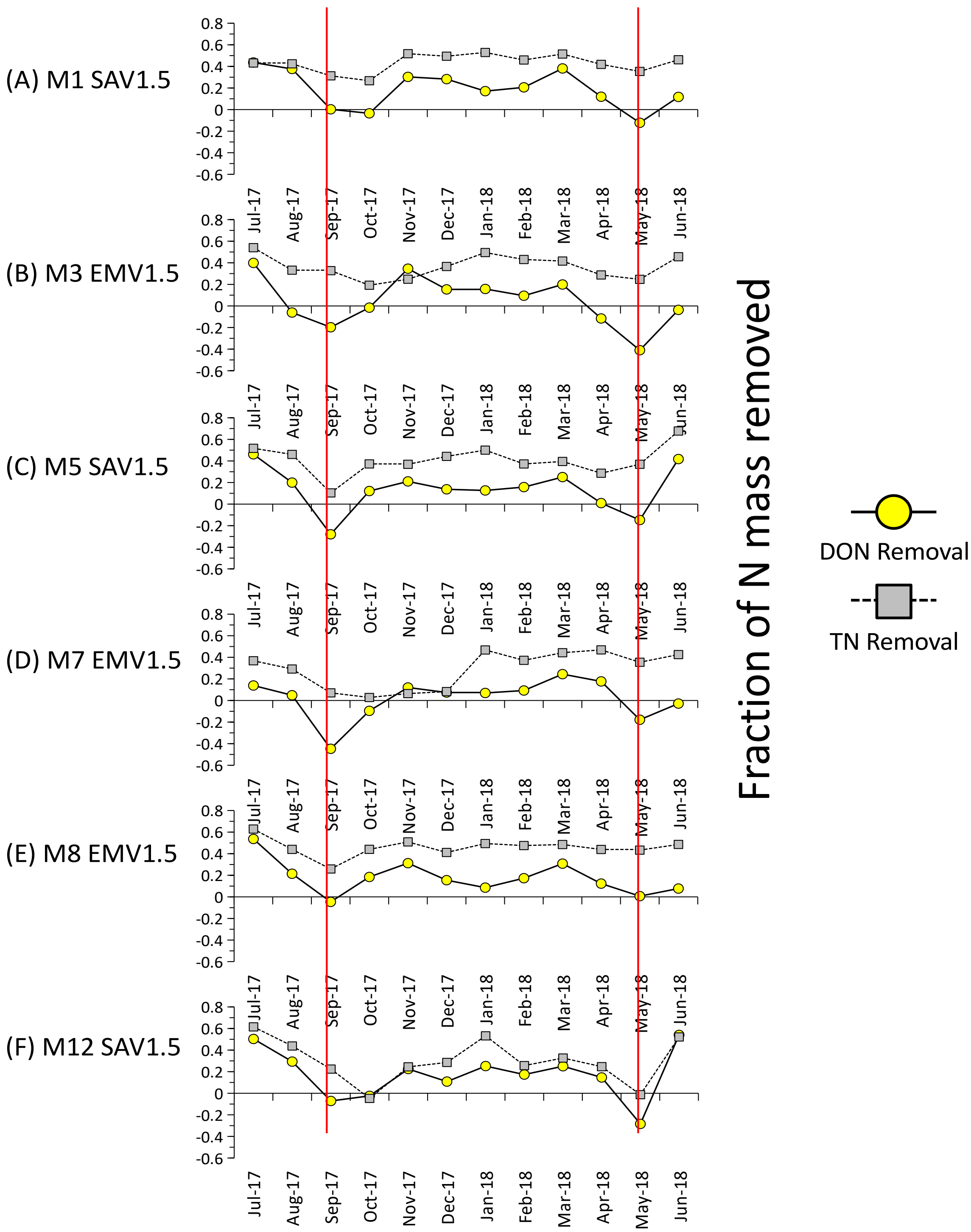

Figure 6. Time series of the monthly fraction of TN (dash with grey square) and DON (solid with yellow circle) for each of the six HLR 1.5 cm d^{-1} mesocosms. (A) M1, (B)M3, (C) M5, (D) M7, (E) M8, (F) M12. Red lines marks depressing in N removal in Sept 2017 and May 2018.

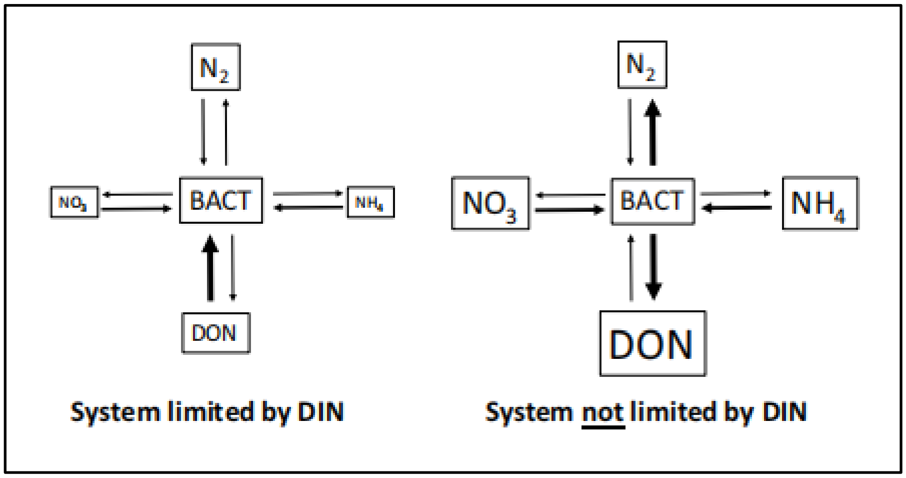

Figure 7. Conceptual model of microbially mediated N cycling to explain DON patterns in the mesocosms (Pisani et al., 2017).

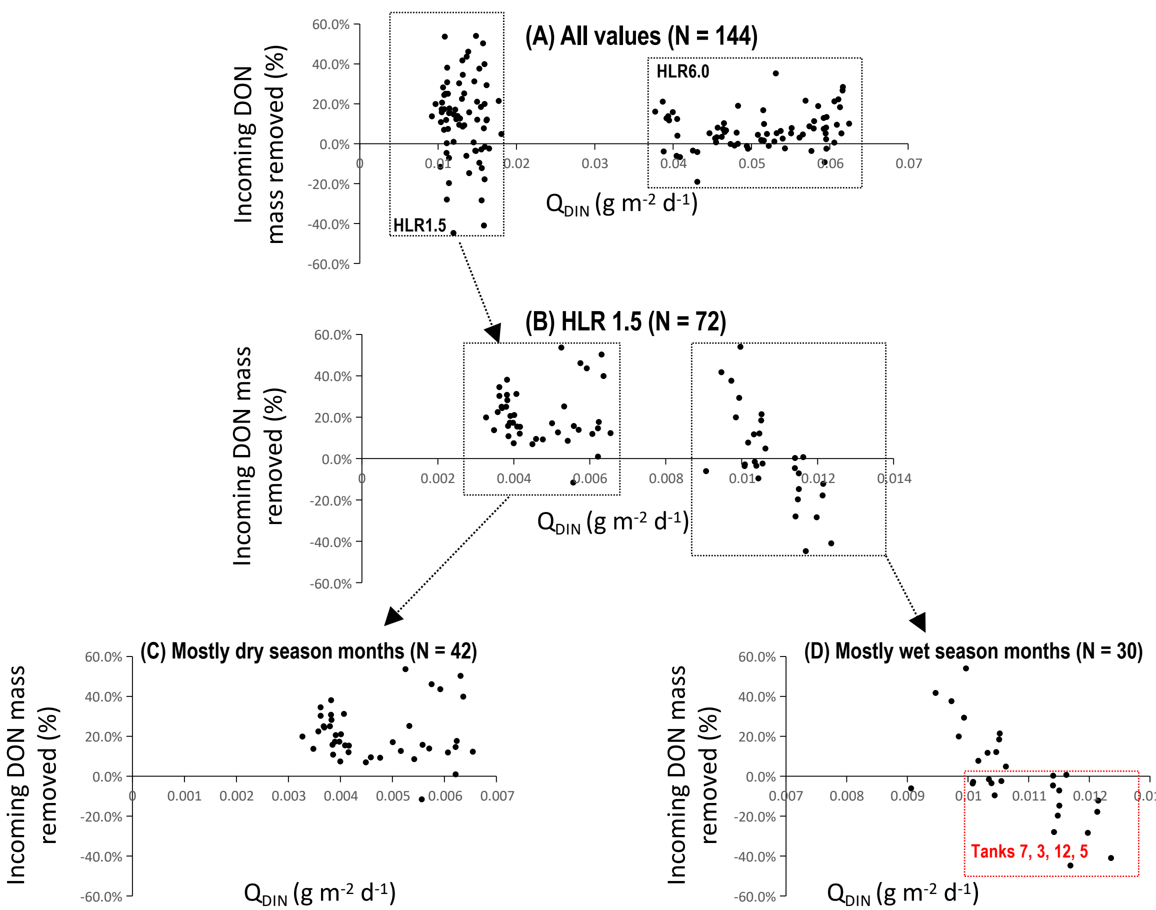

Figure 8. Scatterplots of DIN loading (QDIN; g m-2 d^{-1}) vs. the percentage in incoming DON removed. (A) All months and mesocosms (N = 144). (B) HLR 1.5 cm d^{-1} mesocosms only (N = 72). (C and D) Zoomed sub-sets of HLR 1.5 cm d^{-1}.

Figure 9. Hypothesized relationships between incoming N load and N removal over a range of HLR values. Q_{TN} vs. TN removed (ΔTN) on top and left axes in blue. Q_{DIN} vs. DON removed (ΔDON) on bottom and right axes in red. The optimal range for HLR should be 6-8 cm d^{-1}.

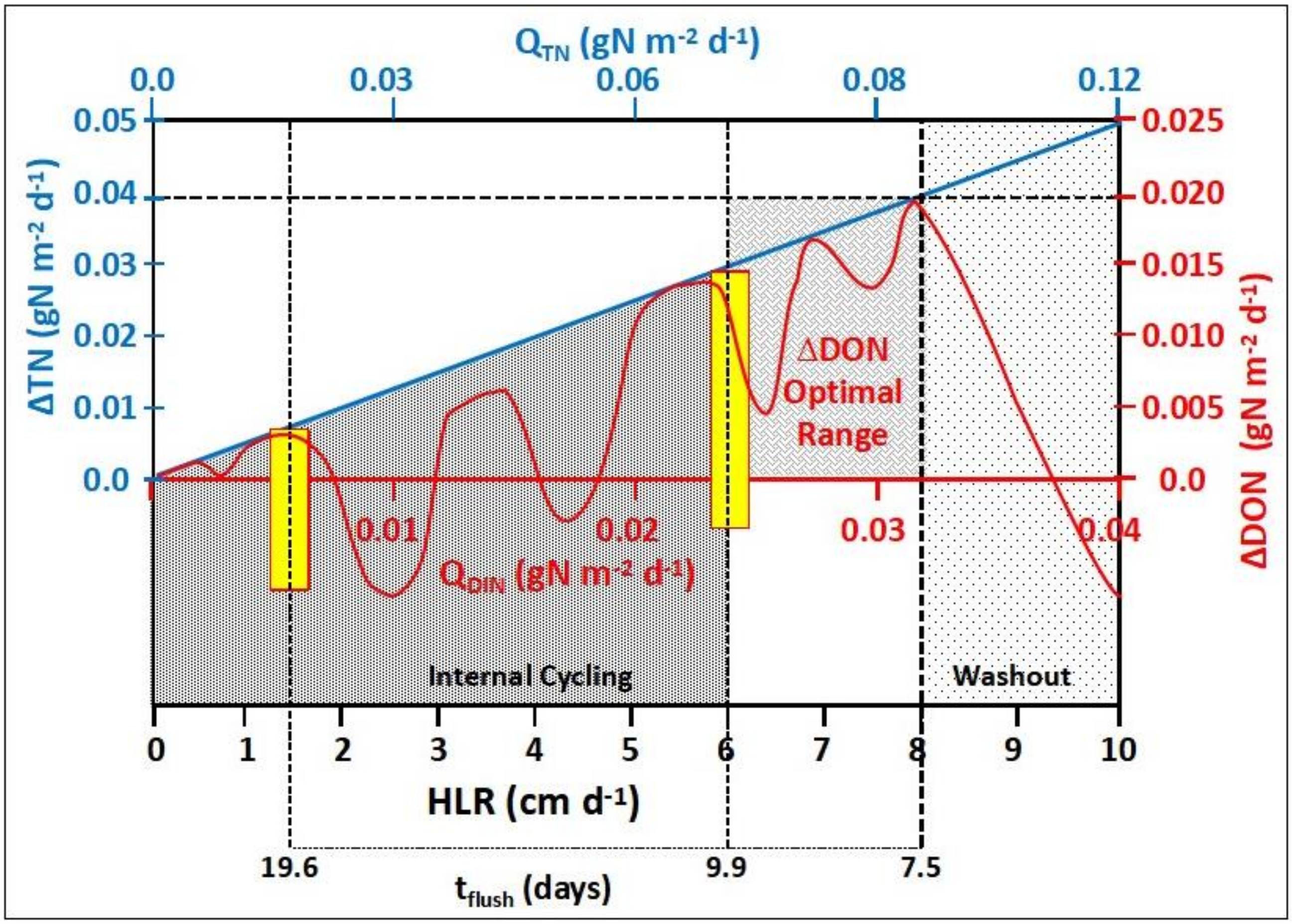

4.5 Mass Balance N Budgets

4.5.1 Approach

The conceptual model in Figure 3 served as the basis for eight separate N budgets representing dry and wet season examples for each combination of plant community (EMV vs. SAV) and HLR (1.5 vs. 6.0 cm d^{-1}). The data from the N Removal and N Cycling components were merged with estimated values for pools and process which were not determined in the mesocosms. The data from the mesocosms included the TN inputs and outputs, the N masses in the water column, the composition of TN for both inputs and outputs, the total N in the sediment, the porewater concentrations (DON, NH_4^+, NO_X^-), the sediment-water exchanges (SWX), and denitrification rates (Cornwell et al., 2019; J-Tech, 2019). The N contents, uptake, and organic production by phytoplankton, periphyton, and plants were derived through a combination of mesocosm data and literature values for Everglades wetlands. Nitrogen transformation rates were derived using a combination of measured organic N remineralization rates (Cornwell et al., 2019) and basal metabolic rates (d^{-1}) commonly utilized in water quality models (Buzzelli et al., 2014; Gajewska and Skrzypiec, 2018).

4.5.2 N Inputs and Outputs

The N budgets used the seasonal change in TN (ΔTN; gN $season^{-1}$) observed in the N Removal component of the C43WTTP study as the target amount of N against which to compare the sum of the internal changes during the mass balance process. The percentages of the 4 constituents (DON, NH_4^+ NO_x^-, PN) derived from the header tanks were used to split TN from HLR (TN_{HLR}) into four separate inputs (Figure 3; Table 3). These same percentages were used to divide the TN input from rain (TN_{rain}) among the four constituents. The mass of TN observed in the outflow (TN_{OUT}) also was divided similar into the 4 constituents but based on the ratios from the water within the mesocosms (Table 3).

The individual inputs and outputs for each mesocosm were summed seasonally and then averaged for each combination of plant and HLR (Table 4). The average seasonal amounts of input and output for each constituent were divided by 182.5 to derive daily values (g N d^{-1}). Since HLR was a controlled treatment, the load of N from the header tanks varied due to differences in the incoming concentration between dry and wet seasons. In contrast, N input from rain increased 7-10 times between dry and wet seasons. However, all 12 mesocosms received the same rainfall and thus the same atmospheric load of N each season (Table 4).

4.5.3 Water Column N

The average concentrations of DON (~1.0 mg L^{-1}), NH_4^+ (~0.02 mg L^{-1}), and NO_x^- (~ 0.004 mg L^{-1}) in the water column were consistent among the eight different combinations of vegetation, HLR, and season (Table 5). These concentrations were converted to their constituent masses in the water column pools (gN) using a unit conversion (1 mg L^{-1} = 1 g m^{-3}) and multiplying by the average volumes (m^3) of the mesocosms (V_{EMV} = 7.1 m^3; vs. V_{SAV} = 3.65 m^3; Table 6).

4.5.4 Sediment N

Total sediment N content in the upper 1 cm (0.01 m) was 18.5 ±16.3 g m^{-2}, 14.8 ±10.1 g m^{-2}, 8.4 ±7.6 g m^{-2}, and 4.8 ±2.4 g m^{-2} among the EMV 1.5 cm d^{-1}, EMV 6.0 cm d^{-1}, SAV 1.5 cm d^{-1}, and SAV 6.0 cm d^{-1} budgets in both dry and wet seasons (Table 5; (Cornwell et al., 2019). The sediment surface layer N mass (gN) was calculated by multiplying the concentration (gN gdw $sediment^{-1}$) by the sediment bulk density (gdw m^{-2}) and the mesocosm surface area (A_{meso}; 11.9 m^2). Porewater DON ranged from 103.0 ±126.7 µM to 175.3 ±84.2 µM. The average NH_4^+ concentrations in the porewater from the EMV tanks (125.3 ±225.7 and 103.5 ±63.7 µM) were much less than those from the SAV tanks (458.0 ±212.0 and 618.1 ±446.8 µM). The concentrations of NO_x^- were variable ranging from 0.4 ±0.4 µM to 1.2 ±1.6 µM (Table 5). The masses of DON, NH_4^+, and NO_x^- in the porewater (gN) were calculated using a unit conversion (1 µM = 0.014 gN m^{-3}) and multiplying the resulting concentrations by the 0.02 m sediment surface layer thickness, the sediment water content, and A_{meso} (Cornwell et al., 2019).

4.5.5 Sediment-Water Exchanges

Rates of NH_4^+ efflux from the sediment ranged from 0.001 g N d^{-1} (EMV 1.5 cm d^{-1}dry) to 0.035 g N d^{-1} (SAV 6.0 cm d^{-1} wet; Table 7). The influx of NO_x^- to the sediment was of similar magnitude ranging from 0.001-0.017 g N d^{-1}. Mass rates were 2-5 times greater in the wet relative to the dry season for both NH_4^+ efflux and NO_x^- influx. The efflux of N_2-N from the sediments ranged from 0.005-0.035 g N d^{-1} and were generally greater in the wet season. The only exception was the SAV 1.5 cm d^{-1} budget where the rate of N_2-N efflux in the wet season (0.006 g N d^{-1}) was slightly less than that in the dry season (0.01 g N d^{-1}). DON exchange between the sediments and water was the least predictable and most variable among the eight different cases. DON mass was removed from the water column in EMV 1.5 cm d^{-1}dry, EMV 6.0 cm d^{-1}wet, SAV 1.5 cm d^{-1}wet, and SAV 6.0 cm d^{-1} wet season budgets (Table 7). Conversely, the sediment was a source of DON for other four N budgets (EMV 6.0 cm d^{-1} dry, EMV 1.5 cm d^{-1} wet, SAV 1.5 cm d^{-1} dry, and SAV 6.0 cm d^{-1} dry).

4.5.6 Phytoplankton, Periphyton, and Plants

The N pools and processes related to phytoplankton, periphyton, and plants were not formally determined in the mesocosms. Qualitative data on the composition and biomass in the mesocosms was coupled with literature information to estimate the N demand for primary production and its contribution to internally produced PN (Table 8). Evaluation of the mesocosm information, literature values, and estimated N pool sizes led to the adoption of a steady-state assumption for N demand and loss by phytoplankton, algae, periphyton, and plants.

Conversion of the average chlorophyll *a* concentration from within the mesocosms was used to establish the steady-state N pool size for phytoplankton (N_{phyto}; gN). Overall, chlorophyll *a* in the water column of the tanks ranged from 2.6±2.7 µg L^{-1} (EMV 1.5 Wet) to 15.2±18.1 µg L^{-1} (SAV 1.5 Wet; Table 5). The mass of N in phytoplankton was calculated using a unit conversion (1 µg L^{-1} = 1 mg m^{-3}), multiplying the resulting value by the ratio of carbon to chlorophyll *a* (50 gC $gCHL^{-1}$; Cloern et al., 1996), and dividing it by the molar C:N ratio (6.6 moles C mole N^{-1}). Maintenance of steady-state phytoplankton N mass required that the amount of N for growth equaled the amount of loss each day. The phytoplankton growth (and loss) rate was assumed to be 0.01 d^{-1} (Buzzelli et al., 2014). This value was multiplied by N_{phyto} to estimate the daily amount of DIN removed from the water column (uptake) as well as the daily amount of N mass lost to the internal PN pool.

The steady-state masses of N contained in EMV and SAV (N_{plant}; gN; Table 8) were estimated through a combination of the total dry weight biomass determined at the end of the study, interpretation of the visual percent cover noted during the mesocosm study, and literature values for N tissue contents (Chimney and Pietro, 2006; Chiang et al., 2000; Craft et al., 1995; McJannet et al., 1995; Vaithiyanathan and Richardson, 1998; Vermeer et al., 2003; Wozniak et al., 2015; J-Tech ,2019). The target steady-state, dry weight biomass for both EMV and SAV mesocosms was determined to be 2000 gdw m^{-2}. The N contents of *Utricularia*, algae, and periphyton were pooled for N_{algae} with the N contents of the vascular plants pooled for N_{plant}. The resulting sizes of the algal and plant N pools were 71.4 gN (EMV algae), 19.0 gN (EMV plant)35.7 gN (SAV algae), and 480.8 gN (SAV plant; Table 8).

Similar to phytoplankton, the maintenance of steady-state N mass required that the amount of N for growth equaled the amount of loss each day. Thus, it was assumed that net annual primary production in the mesocosms via contributions of algae, periphyton, *Utricularia*, and different macrophytes (EMV = *Typha*, *Eleocharis*, *Schoenoplectus*; SAV = *Najas* and *Chara*) was 2000 gdw m^{-2} y^{-1}. This estimate was within measured rates of primary production in periphyton and macrophyte dominated Everglades wetlands (Ewe et al., 2006; Hagerthey et al., 2010). The total of 2000 gdw m^{-2} y^{-1} was divided into the relative fractions among the primary producers using the estimated percentages, converted to N using the differential N contents (gN gdw^{-1}), multiplied by the area of the mesocosms (11.9 m^2), and then divided by 365 to derive daily rates (g N d^{-1}) of N demand (e.g. N uptake) and N loss to detrital PN.

4.5.7 Nitrogen Transformations

Several key N transformation processes were not directly measured in the mesocosms. These processes included the hydrolysis of PN to produce DON in the water and sediments, the production of NH_4^+ from DON (ammonification), and the internal generation of NO_X^- (nitrification) which is essential for coupled denitrification (Cornwell et al., 1999; Figure 3). Although divided into components for the N budgets, all of these processes are part of organic mineralization and denitrification (Cornwell et al.; 2019). The calibration process relied on the net remineralization rates from the N Cycling study as a reference while parameters were introduced to establish the budgets. The magnitude of the transformation rates were also compared to the total N loss coefficient reported in Gajewska and Skrzypiec (2018; 0.007 m d^{-1}) following unit conversion using the average water height in the mesocosms (~0.01 d^{-1}). This process resulted in a group of six N parameters for all eight N budgets (Table 9).

It was assumed that 55% of the total PN pool would undergo hydrolysis to produce DON (f_{hydrol} = 0.55; Buzzelli et al., 2014). This means that 45% was refractory and did not contribute to N cycling. The basal rate at which PN was hydrolyzed to DON (0.005 d^{-1}) was adopted based on previous water quality models (k_{hydrol}; Buzzelli et al., 2014). The loss term for the PN pool via hydrolysis had to be divided into separate DON sources for the water and sediments. Therefore 20% of the N resulting from PN hydrolysis was put into the water column DON pool with the remaining 80% added to the sediment.

The average rate of remineralization determined by Cornwell et al., (2019; 0.008 d^{-1}) was multiplied by the masses of the DON pools in the water and sediment to approximate ammonification. Similarly, nitrification served as a NH_4 loss term in the water and sediment and the NO_X source term using a basal rate of 0.001 d^{-1} multiplied by the masses of the NH_4 pools (Buzzelli et al., 2014). The rate of N-N_2 efflux from the sediments was assumed to represent the loss of NO_X through denitrification. Finally, 80% of the phytoplankton N requirement was assumed to be through NH_4 uptake with the remaining 20% from the NO_X pool (Table 9).

4.5.8 N Budget Attributes and Mass Balance

Most of the N was located in the algae (6-19% of total), plants (29-82% of total), and PN (8-53% of total; Figure 10 to Figure 13). A greater amount was contained in algae and PN in the EMV relative to the SAV where the plant N pool was the largest at 480.8 gN (Figures 12-13). Water column DON was the largest dissolved pool and was nearly double the mass in the SAV (6.5-6.8 gN) compared to the EMV (2.8-3.6 gN) budgets. While the sediment DON and NH_4^+ pools were of similar magnitude among the EMV budgets (0.103-0.174 gN), there was 2-5X more NH_4^+ than DON in the sediments of the SAV budgets

(0.20 vs. 0.57 gN). Denitrification was in excess of combined external NO_x^- loading and internal nitrification in all 8 budgets. While denitrification represented a net loss of N from the wetland, rates of N uptake by algae + periphyton and plants was 10-100 times greater. Internal production and material cycling maintain N within the ecosystem (Messer et al., 2017). The biggest difference among all N budgets was the sediment-water DON exchange which ranged from -0.05 gN d^{-1} for sediment influx to 0.36 gN d^{-1} for sediment efflux with no relationship to plant community, HLR, or season.

The calibration of initial N budgets resulted in surplus of DON. Although photolysis was not considered to be important, it was included in the conceptual model as a potential loss term for DON (Figure 3; Gryzbowski and Tranvik, 2008). The results of Pisani et al., (2017) indicated that while light exposure did not directly affect the production of bioavailable DON, it could alter the composition and concentration of total DON in the C-43 Canal. Thus, photolysis was introduced as a loss term for DON to balance the N budgets.

DON loss through photolysis (gN d^{-1}) was calculated by multiplying the daily loss rate (k_{phytol}; d^{-1}) by the DON masses in the water column and sediment. The initial value for the photolytic constant (0.025 d^{-1}) equaled 2.5% of the DON pools lost each day (Table 10). The value for k_{photol} was increased to 0.15 d^{-1} and 0.10 d^{-1} for the EMV 6.0 cm d^{-1} dry and wet season budgets, respectively. These were the greatest daily fractions of DON loss (10-15%) required for the $N_{cycling}$ to approximate N_{remove}. For example, when 10% of the DON was removed daily through photolysis in the SAV 1.5 cm d^{-1} dry season budget, the sum of internal cycling (15.9 gN $season^{-1}$) nearly equaled the target TN removal (16.1 gN $season^{-1}$; Table 10)). However, internal cycling only accounted for 81.7% of the target for the SAV 1.5 cm d^{-1} wet season budget with the same DON loss rate. The four budgets with DON influx (EMV 6.0 cm d^{-1} wet , EMV 1.5 cm d^{-1} dry, SAV 1.5 cm d^{-1} wet, and SAV 6.0 cm d^{-1} wet) overestimated the total amount of TN removal by 2.3-7.3% because of internal DON consumption. Conversely, total TN removal was underestimated because of DON efflux from the sediment in the other four budgets (EMV 6.0 cm d^{-1} dry, EMV 1.5 cm d^{-1} wet, SAV 1.5 cm d^{-1} dry, and SAV 6.0 cm d^{-1} dry).

Table 4. Summary of inflow or hydraulic loading rate (HLR), rainfall (RAIN), and outflow (OUT) for each combination of plant community (EMV vs. SAV) and hydraulic loading rate (HLR 1.5 vs. 6.0 cm d^{-1}) for mesocosm N budgets. All values in g N d^{-1}.

Plant	HLR	Season	DON			NH_4			NO_X			PN		
			HLR	RAIN	OUT	HLR	RAIN	OUT	HLR	RAIN	OUT	HLR	RAIN	OUT
EMV	1.5	Dry	0.191	0.009	0.122	0.004	0.0002	0.002	0.0007	3.1×10^{-5}	0.0004	0.021	0.001	0.015
EMV	1.5	Wet	0.193	0.076	0.176	0.005	0.0019	0.004	0.0006	2.3×10^{-4}	0.0005	0.028	0.011	0.025
EMV	6.0	Dry	0.805	0.010	0.546	0.016	0.0002	0.011	0.0047	5.6×10^{-5}	0.003	0.049	0.001	0.041
EMV	6.0	Wet	0.799	0.077	0.584	0.020	0.0019	0.014	0.0034	3.3×10^{-4}	0.002	0.103	0.010	0.077
SAV	1.5	Dry	0.178	0.009	0.110	0.003	0.0002	0.002	0.0011	5.4×10^{-5}	0.0006	0.027	0.001	0.019
SAV	1.5	Wet	0.161	0.064	0.144	0.004	0.0015	0.003	0.0004	1.7×10^{-4}	0.0004	0.059	0.023	0.055
SAV	6.0	Dry	0.765	0.009	0.540	0.017	0.0002	0.012	0.0027	3.2×10^{-5}	0.0019	0.073	0.001	0.052
SAV	6.0	Wet	0.768	0.074	0.590	0.027	0.0026	0.021	0.0022	2.1×10^{-4}	0.0016	0.127	0.012	0.098

Table 5. Summary concentrations for the water column variables (mg L^{-1}), total sediment nitrogen (g m^{-2}) and molar C:N, and porewater nitrogen (µM) for each combination of plant community (EMV vs. SAV) and hydraulic loading rate (HLR 1.5 vs. 6.0 cm d^{-1}) for mesocosm N budgets. The total sediment N was calculated for the top 1 cm. Porewater concentrations were from the 2 cm section of the equilibrators (Cornwell et al., 2019).

Plant	HLR	Season	Water Column (mg L^{-1})				Sed Total (g m^{-2})		Sed PW (µM)		
			DON	NH_4	NO_X	CHL	N	CN	DON	NH_4	NO_X
EMV	1.5	Dry	1.01±0.18	0.02±0.007	0.004±0.002	7.5±14.9	18.5±16.3	12.5±1.3	142.9±64.2	125.3±225.7	1.2±1.6
EMV	1.5	Wet	0.97±0.15	0.02±0.014	0.003±0.001	10.3±11.3					
EMV	6	Dry	0.80±0.24	0.02±0.008	0.005±0.005	2.6±2.7	14.8±10.1	11.8±1.8	175.3±84.2	103.5±63.7	0.8±1.2
EMV	6	Wet	0.84±0.26	0.02±0.007	0.004±0.002	4.6±5.1					
SAV	1.5	Dry	0.96±0.10	0.02±0.009	0.005±0.005	9.5±10.4	8.4±7.6	12.3±3.0	159.1±116.0	458.0±212.0	0.4±0.4
SAV	1.5	Wet	0.95±0.16	0.02±0.014	0.003±0.001	15.2±18.1					
SAV	6	Dry	0.96±0.08	0.02±0.010	0.003±0.002	8.6±6.1	4.8±2.4	13.5±3.1	103.0±126.7	618.1±446.8	0.6±0.9
SAV	6	Wet	1.02±0.12	0.04±0.029	0.003±0.003	7.5±5.6					

Table 6. Summary of masses of N pools for each combination of plant community (EMV vs. SAV) and hydraulic loading rate (HLR 1.5 vs. 6.0 cm d^{-1}) for mesocosm N budgets. All values in g N.

Plant	HLR	Season	Phyto	Algae	Plant	PN	DON_w	$NH4_w$	NOX_{sw}	DON_s	$NH4_s$
EMV	1.5	Dry	0.45	71.4	119.0	220.2	3.56	0.070	0.0136	0.142	0.124
EMV	1.5	Wet	0.61	71.4	119.0	220.2	3.38	0.083	0.0116	0.142	0.124
EMV	6.0	Dry	0.13	71.4	119.0	175.4	2.86	0.059	0.0178	0.174	0.103
EMV	6.0	Wet	0.25	71.4	119.0	175.4	2.98	0.071	0.0128	0.174	0.103
SAV	1.5	Dry	0.29	35.7	480.8	100.1	6.75	0.122	0.0397	0.197	0.566
SAV	1.5	Wet	0.46	35.7	480.8	100.1	6.57	0.150	0.0182	0.197	0.566
SAV	6.0	Dry	0.27	35.7	480.8	56.8	6.75	0.149	0.0242	0.127	0.764
SAV	6.0	Wet	0.26	35.7	480.8	56.8	7.15	0.252	0.0207	0.127	0.764

Table 7. Summary of sediment-water exchange rates (g N d^{-1}) for each combination of plant community (EMV vs. SAV) and hydraulic loading rate (HLR 1.5 vs. 6.0 cm d^{-1}) for mesocosm N budgets. Negative values denote removal of material from water column to sediment.

Plant	HLR	Season	DON_{SWX}	$NH_{4\ SWX}$	$NO_{X\ SWX}$	$N_{2\ SWX}$
EMV	1.5	Dry	-0.058	0.001	-0.003	0.005
EMV	1.5	Wet	0.358	0.006	-0.012	0.034
EMV	6.0	Dry	0.118	0.007	-0.001	0.014
EMV	6.0	Wet	-0.055	0.018	-0.011	0.024
SAV	1.5	Dry	0.094	0.002	-0.003	0.010
SAV	1.5	Wet	-0.049	0.010	-0.017	0.006
SAV	6.0	Dry	0.061	0.007	-0.006	0.011
SAV	6.0	Wet	-0.039	0.035	-0.011	0.035

Table 8. Biomass and nitrogen contents for primary production in the mesocosms. A value of 2000 gdw m^{-2} was determined to be the steady state condition for primary production in both EMV and SAV. The relative proportions among the dominant taxa were determined from a combination of mesocosm percent cover data and personal observations. The N contents were derived from several literature sources (Chimney and Pietro, 2006; Chiang et al., 2000; Craft et al., 1995; McJannet et al., 1995; Vaithiyanathan and Richardson, 1998; Vermeer et al., 2003; Wozniak et al., 2015). The N contents of *Utricularia*, algae, and periphyton were pooled to estimate N Algae and the N contents of the vascular plants were pooled to estimate N Plant for use in N budgets.

	%Biomass	gN gdw^{-1}	gN m^{-2}	N_{Algae}	N_{Plant}
EMV				71.4	119.0
Utricularia	0.15	0.010	3.0		
Algae + Periphyton	0.10	0.015	3.0		
Typha	0.25	0.006	3.0		
Eleocharis	0.25	0.007	3.5		
Schoenoplectus	0.25	0.007	3.5		
SAV				35.7	480.8
Najas	0.50	0.030	30.0		
Chara	0.40	0.013	10.4		
Algae + Periphyton	0.10	0.015	3.0		

Table 9. Values for parameters used in mesocosm N budgets. Initial values derived from Buzzelli et al., (2014a) and Cornwell et al., (2019) and specified through the development of the mesocosm N budgets.

Parameter	Definition	Unit	Value
f_{LPN}	Labile fraction of PN	unitless	0.55
k_{hydrol}	Hydrolysis rate of PN	d^{-1}	0.005
f_{hydrol}	Fraction of PN hydrolysis to DON_w	unitless	0.2
k_{amm}	Ammonification rate	d^{-1}	0.008
k_{nit}	Nitrification rate	d^{-1}	0.001
f_{NHup}	NH4 fraction of algal N uptake	unitless	0.80

Table 10. Summary of the effects of DON photolysis in the calibration and mass balance of the N budgets. The magnitude of the photolysis parameter (k_{photol}) was varied for each of the 8 N budgets to balance DON sources vs. sinks, affect the calculated sum of internal changes ($N_{cycling}$) and better approximate the target total seasonal mass removal (N_{remove}). The final column provides the difference between these two calculations and represents either an under- (negative) or over-estimate (positive) of the target seasonal removal.

Plant	HLR	Season	k_{photol} d^{-1}	N_{Remove} gN $season^{-1}$	$N_{Cycling}$ gN $season^{-1}$	ΔN MB gN $season^{-1}$
EMV	1.5	Dry	0.025	16.0	18.3	+2.3
EMV	1.5	Wet	0.025	19.9	24.5	+4.6
EMV	6.0	Dry	0.150	51.8	59.1	+7.3
EMV	6.0	Wet	0.100	61.2	63.9	+2.3
SAV	1.5	Dry	0.010	16.1	15.9	-0.2
SAV	1.5	Wet	0.010	20.2	16.5	-3.7
SAV	6.0	Dry	0.035	47.9	47.1	-0.9
SAV	6.0	Wet	0.035	55.4	58.9	-0.5

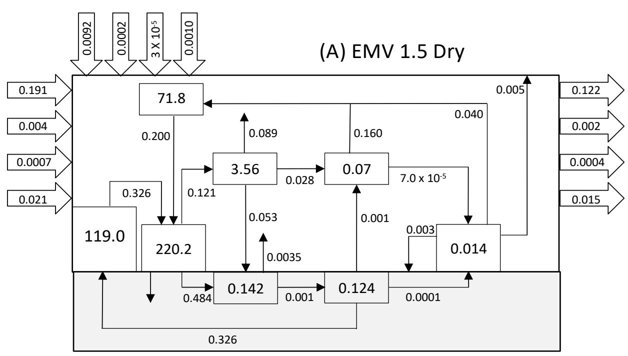

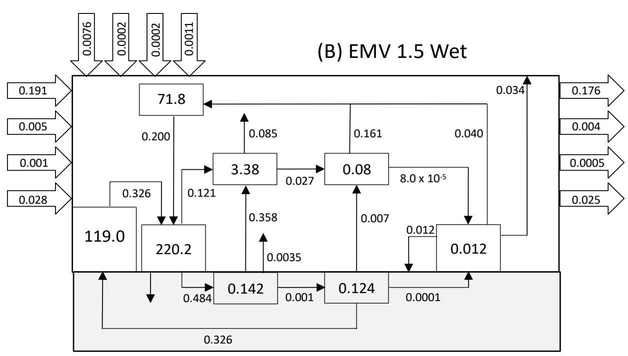

Figure 10. Nitrogen budgets for the EMV 1.5 example. (A) EMV 1.5 cm d^{-1} Dry. (B) EMV 1.5 cm d^{-1} Wet. The sediment was a sink for water column DON in the dry season but a source in the wet season.

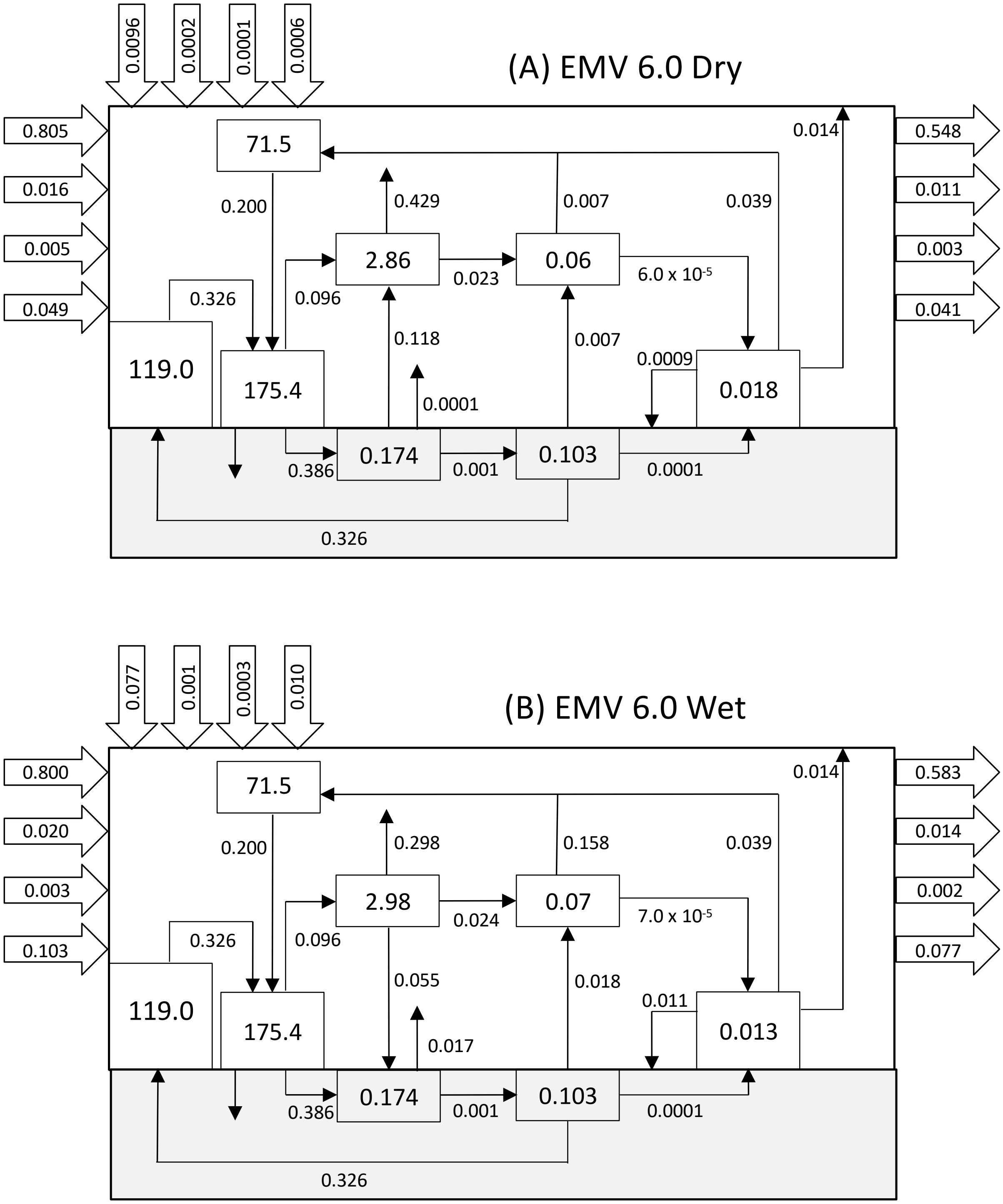

Figure 11. Nitrogen budgets for the EMV 6.0 example. (A) EMV 6.0 Dry. (B) EMV 6.0 Wet. The sediment was a source for water column DON in the dry season but a sink in the wet season.

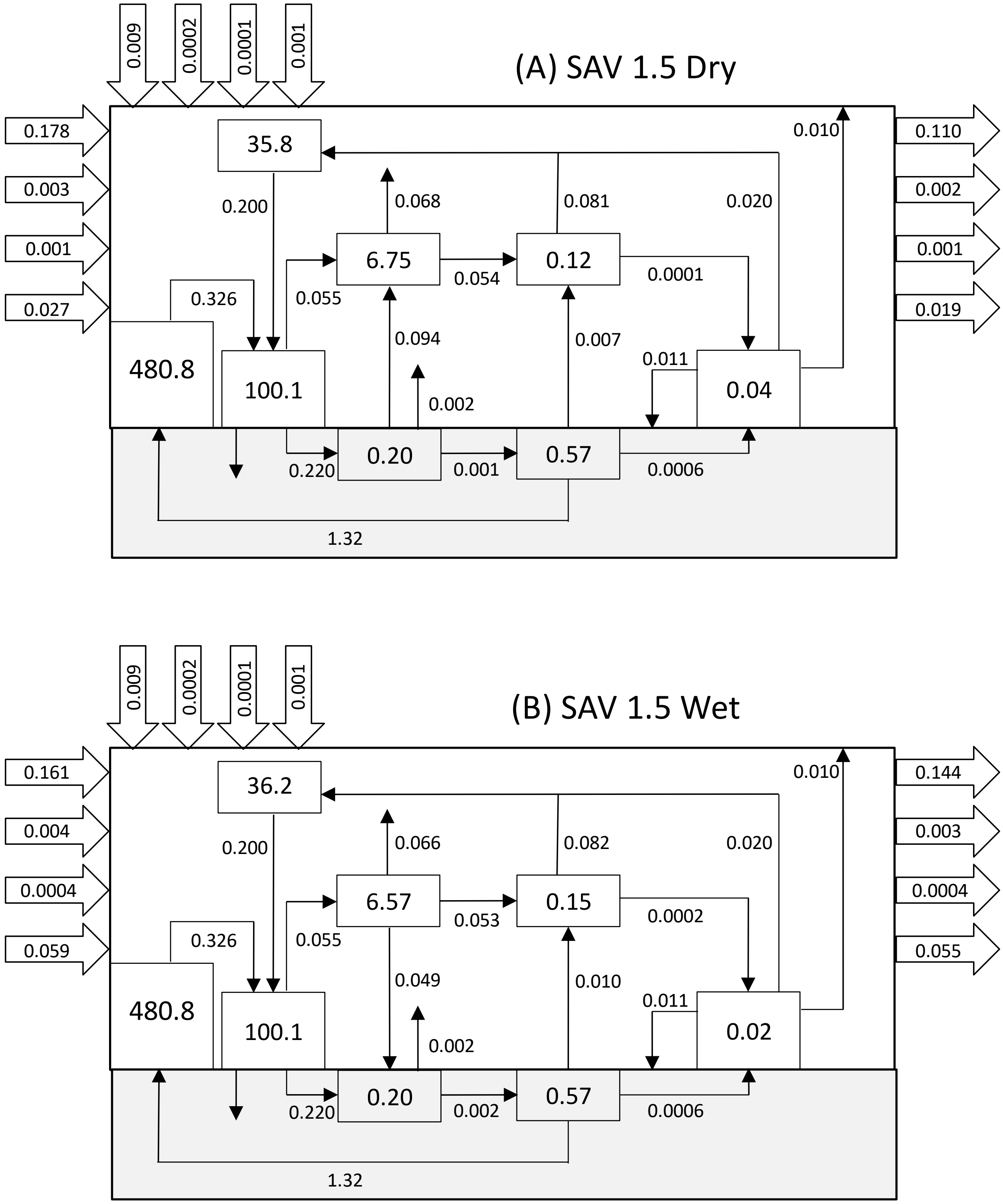

Figure 12. Nitrogen budgets for the SAV 1.5 example. (A) SAV 1.5 Dry. (B) SAV 1.5 Wet. The sediment was a source for water column DON in the dry season but a sink in the wet season.

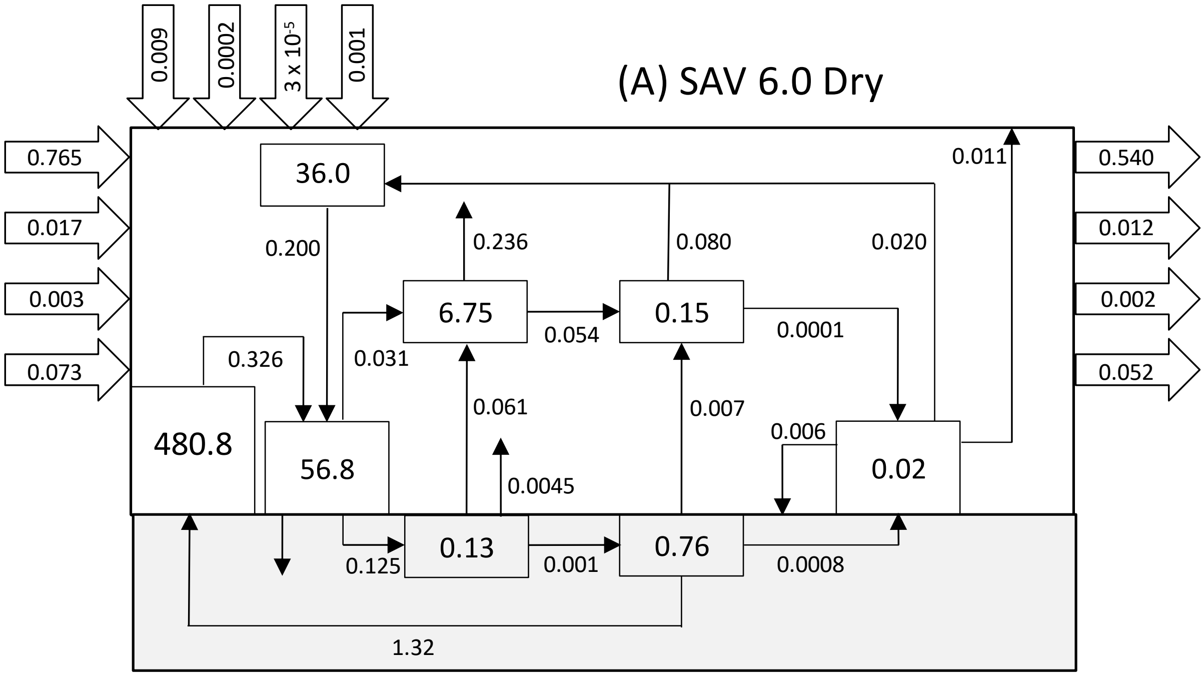

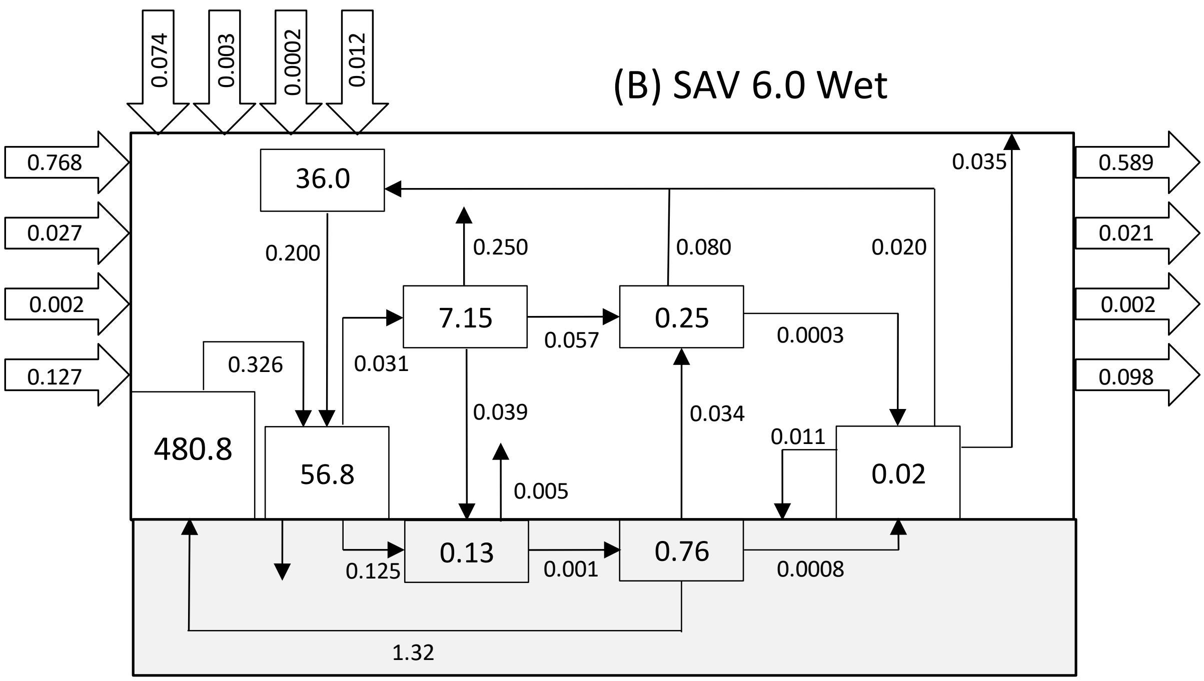

Figure 13. Nitrogen budgets for the SAV 6.0 example. (A) SAV 6.0 Dry. (B) SAV 6.0 Wet. The sediment was a source for water column DON in the dry season but a sink in the wet season.

5 Project Summary and Recommendations for Phase II

5.1 Project Summary

A conceptual model of wetland N cycling was created to integrate the physical inputs/outputs of TN (N Removal) with the internal changes due to N transformations in the water and sediments (N Cycling). This approach resulted in a computational scheme to account for the TN removed using the sum of the production and consumption among the internal N pools. The balancing of all N sources vs. sinks revealed the importance of DON as a central but variable part of TN removal. Moreover, DON loss became the key process through which to balance the N budgets. The conceptualization resulted in 9 pools and 14 processes based on the study objectives, details of the Phase I data, and state of knowledge for N cycling in freshwater wetlands.

There was a strong linear relationship observed between TN loading and removal with 27-46% of incoming TN removed by the mesocosms annually. However, only 2-20% of the DON was removed over the same period. This occurred because of reduced DON removal in many wet season months for the mesocosms receiving the lower HLR (1.5 cm d^{-1}). Surplus DON can result in aquatic ecosystems where DIN is in excess of the total N required for net productivity. This pattern was not observed in mesocosms with the higher HLR (6.0 cm d^{-1}). Thus, it was hypothesized that a slightly higher HLR (i.e., HLR ≥ 7 cm d^{-1}) may potentially optimize both TN and DON removal by providing the appropriate balance between external DIN loading and internal DON consumption.

Eight N budgets were developed representing each combination of season (dry vs. wet), plant community (EMV vs. SAV), and HLR (1.5 vs. 6.0 cm d^{-1}). The inflows and outflows determined in the N Removal study were connected to the internal pools of water column DON and DIN. Particulate nitrogen (PN) was assumed to be a single internal pool of detrital N located at the sediment-water interface. Similarly, NO_X^- was assumed to be a combined sediment + water N pool because of rapid uptake and denitrification. Algae, plants, and sediments accounted for the remaining N pools. Annual internal primary production was assumed to be in steady state with target biomass estimates for each group. Rates of N transformation in the water and sediments were approximated using calibration parameters.

Most of the N was located in the algae (6-19% of total), plants (29-82% of total), and PN (8-53% of total) among the eight N budgets. Water column DON was the largest dissolved pool and was nearly double in the SAV budgets compared to the EMV budgets. Denitrification was in excess of combined external NO_x^- loading and internal nitrification in all eight budgets. The biggest difference among all N budgets was the sediment-water DON exchange which ranged from -0.05 gN d^{-1} for sediment influx to 0.36 gN d^{-1} for sediment efflux with no relationship to plant community, HLR, or season.

The consumption of DON through photolysis was introduced as a loss term to minimize DON surplus and balance the budgets. The daily rate of photolysis was varied from 1-15% of the internal DON mass during budget calibration to decrease the difference between the target TN removal and the sum of internal cycling. For example, when 10% of the DON was removed daily through photolysis in the SAV 1.5 cm d^{-1} dry season budget, the sum of internal cycling (15.9 gN $season^{-1}$) nearly equaled the target TN removal (16.1 gN $season^{-1}$). However, internal cycling only accounted for 81.7% of the target for SAV 1.5 cm d^{-1} wet season budget with the same DON loss rate. The four budgets with DON influx (EMV 6.0 cm d^{-1} wet

, EMV 1.5 cm d^{-1} dry, SAV 1.5 cm d^{-1} wet, and SAV 6.0 cm d^{-1} wet) overestimated the total amount of TN removal by 2.3-7.3% because of internal DON consumption. Conversely, total TN removal was underestimated because of DON efflux from the sediment in the other four budgets (EMV 6.0 cm d^{-1} dry, EMV 1.5 cm d^{-1} wet, SAV 1.5 cm d^{-1} dry, and SAV 6.0 cm d^{-1} dry).

5.2 Recommendations for Consideration in the Phase II Test Cells Study

Empirical Studies

- Assess primary production and the N contents of algae, periphyton, *Utricularia* sp., and plants to account for all sources of PN, and, sinks for DIN
- Characterize TN and DON and evaluate changes in reactivity under different environmental conditions
- Thoroughly evaluate photolysis and other potential DON loss terms
- N tracer studies at core, mesocosm, or the test cell scale using ^{15}N labeled DIN to determine N rates and track N through the water, algae, plants, and sediments

Simulation Modeling

- Develop a wetland simulation model as an exploratory and management tool to quantify and predict the capacity of the Phase II test cells to filter nutrients
- Assess sources, sinks, and concentration changes over multiple scales of time (days-decades) and space (1-1000 m)
- Predict changes in wetland nutrient storage with changes in water management
- Integrate the information gained in Phase I with new results emerging from the Phase II
- Couple with operations to assess the effects of variable HLR and DIN loading on the N removal efficiency of the wetland test cells

Table 11. Summary of Phase I key findings and recommendations for consideration in the Phase II test cell study

Project Component	Phase I Key Findings	Phase II Recommendations
Exploration of DON dynamics	• 27-46% of TN removed; 2-20 of DON • TN and DON removal equal when DIN gone • More DON with high DIN load & low HLR	• Production of algae, periphyton, plants • Assess composition/reactivity of PN & DON • $^{15}NO_x^-$ dosing study to track test cell N • Consider a higher HLR (i.e., ~7 cm d^{-1}) to optimize DON removal
Development of N Budget	• 8 N budgets (EMV & SAV; 2 HLR; Dry & Wet) • Thoroughly evaluate photolysis and other potential of DON loss terms • Most N = algae, plants, particulate N	• Build simulation model from conceptual • Use model to test variable HLR • Exploration of DON dynamics using model • Extend model domain to STA scale

6 References

Berman, T., and DA.Bronk, 2003. Dissolved organic nitrogen: a dynamic participant in aquatic ecosystems. *Aquatic Microbial Ecology* 31:279-305.

Buzzelli, C., Childers, DL., Dong, Q., and Jones, RD. 2000. Simulation of periphyton phosphorus dynamics in Everglades National Park. *Ecological Modelling* 134(1):103-115.

Buzzelli, C. 2011. Ecosystem Modeling in Small Sub-Tropical Estuaries and Embayment. In: Estuarine and Coastal Ecosystem Modeling, Baird, D., Mehta, A.(eds). Chapter 14, pp. 331-354.

Buzzelli, C., Doering, PH., Wan, Y., Sun, D., and Fugate, D. 2014a. Modeling ecosystem processes with variable freshwater inflow to the Caloosahatchee River Estuary, southwest Florida. I. Model development. *Estuarine, Coastal, and Shelf Science*. 151:256-271.

Buzzelli, C, Gorman, P, Doering, PH, Wan, Y, and Chen, Z. 2015. The application of oyster and seagrass models to evaluate alternative inflow scenarios related to Everglades restoration. *Ecological Modelling* 297:154-170.

Chiang, C, Craft, CB, Rogers, DW., and Richardson, CJ. 2000. Effects of 4 years of nitrogen and phosphorus additions on Everglades plant communities. *Aquatic Botany* 68:61-78.

Chimney, MJ, and Pietro, KC. 2006. Decomposition of macrophyte litter in a subtropical constructed wetland in south Florida (USA). *Ecological Engineering* 27:301-321.

Cloern, JE, Grenz, C, Vidergar-Lucas, L. 1996. An empirical model of the phytoplankton chlorophyll:carbon ratio - the conversion factor betweeen productivity and growth rate. *Limnology & Oceanography* 40(7):1313-1321.

Cornwell, JC., Kemp, WM., and Kana, TM. 1999. Denitrification in coastal ecosystems: methods, environmental controls, and ecosystem level controls, a review. *Aquatic Ecology* 33:41-54.

Cornwell, JC., Owens, M., and Jackson, M. 2019. Direct Measurements of Denitrification Rates in Wetlands Mesocosms: A Comparison of Removal Rates of Biologically Available Nitrogen between Vegetation and Hydraulic Loading Rate Treatments. Final Project Report to the South Florida Water Management District. 103 pg.

Craft, CB, Vymazal, J, and Richardson, CJ. 1995. Response of Everglades plant communities to nitrogen and phosphorus additions. *Wetlands* 15(3):258-271.

Ewe, SML, Gaiser, EE, Childers, DL, Iwaniac, D, Rivera-Monroy, VH, and Twilley, RR. 2006. Spatial and temporal patterns of aboveground net primary productivity (ANPP) along two freshwater-estuarine transects in the Coastal Everglades. *Hydrobiologia* 569L459-474.

FDEP. 2009. Final TMDL Report – Nutrient TMDL for the Caloosahatchee Estuary (WBIDs 3240A, 3240B, and 3240C). Florida Department of Environmental Protection, Tallahassee, FL. September 2009.

Gajewska, M, and Skrzypiec, K. 2018. Kinetics of nitrogen removal processes in constructed wetlands. *E3S Web of Conferences* 26:1-4.

Gribsholt, B Boschker, HTS, Struyf, E, Andersson, M, Tramper, A, De Branbandere, L, van Damme, S, Brion, N, Meire, P, Dehairs, F, Midddleburg, JJ, and Heip, CHR. 2005. Nitrogen processing in a tidal freshwater marsh: A whole ecosystem ^{15}N labelling study. *Limnology & Oceanography* 50(6):1945-1959.

Gryzbowski, W, and Tranvik, L. 2008. Photo transformations of dissolved organic nitrogen. In: Capone, DG, Bronk, DA, Mulholland, MR, Carpenter, EJ (Eds). Nitrogen in the Marine Environment, 2nd Edition, DOI: 10:1016/B978-0-12-3725.22-6.00010-4. pgs 511-528.

Hagerthey, SE, Cole, JJ, and Kilbane, D. 2010. Aquatic metabolism in the Everglades: Dominance of water column heterotrophy. *Limnology & Oceanography* 55(2):653-666.

J-Tech. 2019. Final Project Report for the C-43 Water Quality Treatment and Testing Project (C-43 WQTTP) – Phase I. J-Tech with Wetland Solutions Inc. Final Report to South Florida Water Management District, West Palm Beach, FL. Final Report, August 2019.

Malone, SL, Keough, C, Staudhammer, CL, Ryan, MG, Parton,WJ, Olivas, P, Oberbauer, SF, Schedlbauer, J, and Starr, G. 2015. Ecosystem resistance in the face of climate change: A case study from the freshwater marshes of the Florida Everglades. *Ecosphere* 6(4; A57):1-23.

McJannet, CL, Keddy, PA., and Pick, FR. 1995. Nitrogen and phosphorus tissue concentrations in 41 wetland plants: A comparison across habitats and functional groups. *Functional Ecology* 9(2):231-238.

Messer, TL, Burchell, MR, Bohlke, JK, and Tobias, CR. 2017. Tracking the fate of nitrate through pulse-flow wetlands: A mesocosm scale 15N enrichment tracer study. *Ecological Engineering* 106:597-608.

Owens, MS, and Cornwell, JC. 2016. The benthic exchange of O2, N2 and dissolved nutrients using small core incubations. *Journal of Visual Experiments*. 114, e54098, doi:10.3791/54098.

Pisani, O, Boyer, JN, Podgorski, DC, Thomas, CR, Coley, T, and Jaffe, R. 2017. Molecular composition and bioavailability of dissolved organic nitrogen in a lake flow-influence river in south Florida, USA. *Aquatic Sciences*, 79:891-908.

SFWMD. 2015. Appendix 10-2: Caloosahatchee River Watershed Protection Plan 2015 Update. South Florida Environmental Report Volume I. South Florida Water Management District, West Palm Beach, FL.

SFWMD. 2018. Technical Document to Support Re-evaluation of the Minimum Flow Criteria for the Caloosahatchee River Estuary. Final Report. South Florida Water Management District, West Palm Beach, FL. Available at: https://www.sfwmd.gov/sites/default/files/documents/cre_mfl_tech_doc.pdf

Vaithiyanathan, P., and Richardson, CJ. 1998. Biogeochemical characteristics of the Everglades sloughs. *Journal of Environmental Quality* 27(6):1439-1450.

Veldkamp, H. 1977. Ecological Studies with the Chemostat. In: Alexander M. (eds) Advances in Microbial Ecology, Vol 1. Springer, Boston, MA.

Vermeer, CP, Escher, M., Portielje, R., and deKlein, JJM. 2003. Nitrogen uptake and translocation by Chara. *Aquatic Botany* 76:245-258.

Vyzamal, J. 2016. The use of constructed wetlands for nitrogen removal from agricultural drainage: A review. *Scientia Agriculturae Bohemica* 48(2):82-91.

Walker, WW, and Kadlec, RH. 2011. Modeling phosphorus dynamics in Everglades wetlands and stormwater treatment areas. *Critical Reviews in Environmental Science and Technology* 41(SI)(:430-446.